Although our immunohistochemical and immunoelectron microscopic studies detected TSP-1 in the CE, only slight immunohistochemical staining for TSP-1 was detected just below the LE. Immunoelectron labeling for TSP-1 in the LE confirmed that it was present in low amounts (Fig. 5C). We posit that although limbal basal epithelial cells secrete TSP-1 mainly toward the basal side, it diffuses rapidly into fibrous tissue, corneal stroma, or sclera because the area directly below the LE is devoid of Bowman's layer with an affinity for TSP-1. Regarding the fact that normal keratocytes do not secrete TSP-1,[40] we postulate that the staining in the sclera (Fig. 4A) below the CJE may have diffused from basal cells of the LE and/or fibroblasts in the connective tissues below the CJE. We thus suggest that TSP-1 located below the CE accumulates in Bowman's layer, whereas TSP-1 located below the LE diffuses into peripheral tissues.

In summary, in the human ocular surface epithelium, TSP-1 was secreted by corneal and limbal basal epithelial cells toward the basal side. In this respect, the LE and CE exhibited similar characteristics. In contrast to the LE, TSP-1 accumulated in Bowman's layer just below the CE. The expression pattern of TSP-1 in the CJE is different from the pattern noted in the CE and LE. The presence of TSP-1 in Bowman's layer may be related to corneal avascularity and the migration of corneal epithelial cells; however, the physiological relevance of its unique distribution remains to be elucidated. Investigations of the role of TSP-1 in the ocular surface epithelium are under way in our laboratory.

Acknowledgments

The authors thank Bernie Iliakis, Jeremy Shuman, and all the staff of the Northwest Lions Eye Bank (Seattle, WA) for providing corneas in good condition.

References

1. Schermer A, Galvin S, Sun TT. Differentiation-related expression of a major 64K corneal keratin in vivo and in culture suggests limbal location of corneal epithelial stem cells. *J Cell Biol.* 1986;103:49–62.
2. Eichner R, Bonitz P, Sun T-T. Classification of epidermal keratins according to their immunoreactivity, isoelectric point, and mode of expression. *J Cell Biol.* 1984;98:1388–1396.
3. Klyce SD, Crosson CE. Transport processes across the rabbit corneal epithelium: a review. *Curr Eye Res.* 1985;4:323–331.
4. Huang AJ, Tseng SC, Kenyon KR. Paracellular permeability of corneal and conjunctival epithelia. *Invest Ophthalmol Vis Sci.* 1989;30:684–689.
5. Cursiefen C, Masli S, Ng TF, et al. Roles of thrombospondin-1 and -2 in regulating corneal and iris angiogenesis. *Invest Ophthalmol Vis Sci.* 2004;45:1117–1124.
6. Murthy RC, McFarland TJ, Yoken J, et al. Corneal transduction to inhibit angiogenesis and graft failure. *Invest Ophthalmol Vis Sci.* 2003;44:1837–1842.
7. Shao C, Sima J, Zhang SX, et al. Suppression of corneal neovascularization by PEDF release from human amniotic membranes. *Invest Ophthalmol Vis Sci.* 2004;45:1758–1762.
8. Chang JH, Gabison EE, Kato T, Azar DT. Corneal neovascularization. *Curr Opin Ophthalmol.* 2001;12:242–249.
9. Lin HC, Chang JH, Jain S, et al. Matrilysin cleavage of corneal collagen type XVIII NC1 domain and generation of a 28-kDa fragment. *Invest Ophthalmol Vis Sci.* 2001;42:2517–2524.
10. Folkman J. Endogenous angiogenesis inhibitors. *APMIS.* 2004;112:496–507.
11. Tsubota K, Ugajin S, Hasegawa T, Kajiwara K. Conjunctival brush cytology. *Acta Cytol.* 1990;34:233–235.
12. Kawamoto S, Ohnishi T, Kita H, Chisaka O, Okubo K. Expression profiling by iAFLP: a PCR-based method for genome-wide gene expression profiling. *Genome Res.* 1999;9:1305–1312.
13. Kawasaki S, Kawamoto S, Yokoi N, et al. Up-regulated gene expression in the conjunctival epithelium of patients with Sjogren's syndrome. *Exp Eye Res.* 2003;77:17–26.
14. Okubo K, Hori N, Matoba R, et al. Large scale cDNA sequencing for analysis of quantitative and qualitative aspects of gene expression. *Nat Genet.* 1992;2:173–179.
15. Gipson IK, Spurr-Michaud S, Argueso P, Tisdale A, Ng TF, Russo CL. Mucin gene expression in immortalized human corneal-limbal and conjunctival epithelial cell lines. *Invest Ophthalmol Vis Sci.* 2003;44:2496–2506.
16. Nakamura T, Nishida K, Dota A, Kinoshita S. Changes in conjunctival clusterin expression in severe ocular surface disease. *Invest Ophthalmol Vis Sci.* 2002;43:1702–1707.
17. Baenziger NL, Brodie GN, Majerus PW. Isolation and properties of a thrombin-sensitive protein of human platelets. *J Biol Chem.* 1972;247:2723–2731.
18. Gartner TK, Phillips DR, Williams DC. Expression of thrombin-enhanced platelet lectin activity is controlled by secretion. *FEBS Lett.* 1980;113:196–199.
19. Phillips DR, Jennings LK, Prasanna HR. Ca2+-mediated association of glycoprotein G (thrombin sensitive protein, thrombospondin) with human platelets. *J Biol Chem.* 1980;255:11629–11632.
20. Uno K, Hayashi H, Kuroki M, et al. Thrombospondin-1 accelerates wound healing of corneal epithelia. *Biochem Biophys Res Commun.* 2004;315:928–934.
21. Greenwood JA, Murphy-Ullrich JE. Signaling of de-adhesion in cellular regulation and motility. *Microsc Res Tech.* 1998;43:420–432.
22. Tuszynski GP, Nicosia RF. The role of thrombospondin-1 in tumor progression and angiogenesis. *Bioessays.* 1996;18:71–76.
23. Castle VP, Dixit VM, Polverini PJ. Thrombospondin-1 suppresses tumorigenesis and angiogenesis in serum- and anchorage-independent NIH 3T3 cells. *Lab Invest.* 1997;77:51–61.
24. Bugge TH, Flick MJ, Daugherty CC, Degen JL. Plasminogen deficiency causes severe thrombosis but is compatible with development and reproduction. *Genes Dev.* 1995;9:794–807.
25. Soloway PD, Alexander CM, Werb Z, Jaenisch R. Targeted mutagenesis of Timp-1 reveals that lung tumor invasion is influenced by Timp-1 genotype of the tumor but not by that of the host. *Oncogene.* 1996;13:2307–2314.
26. Raugi GJ, Mumby SM, Abbott-Brown D, Bornstein P. Thrombospondin: synthesis and secretion by cells in culture. *J Cell Biol.* 1982;95:351–354.
27. Jaffe EA, Ruggiero JT, Leung LK, Doyle MJ, McKeown-Longo PJ, Mosher DF. Cultured human fibroblasts synthesize and secrete thrombospondin and incorporate it into extracellular matrix. *Proc Natl Acad Sci USA.* 1983;80:998–1002.
28. Jaffe EA, Ruggiero JT, Falcone DJ. Monocytes and macrophages synthesize and secrete thrombospondin. *Blood.* 1985;65:79–84.
29. Hiscott P, Seitz B, Schlötzer-Schrehardt U, Naumann GO. Immunolocalisation of thrombospondin 1 in human, bovine and rabbit cornea. *Cell Tissue Res.* 1997;289:307–310.
30. Lahav J. The functions of thrombospondin and its involvement in physiology and pathophysiology. *Biochim Biophys Acta.* 1993;1182:1–14.
31. Bornatein P. Diversity of function is inherent in matricellular proteins: an appraisal of thrombospondin 1. *J Cell Biol.* 1995;130:503–506.
32. Raugi GJ, Mumby SM, Ready CA, Bornstein P. Location and partial characterization of the heparin-binding fragment of platelet thrombospondin. *Thromb Res.* 1984;36:165–175.
33. Lahav J, Lawler J, Gimbrone MA. Thrombospondin interactions with fibronectin and fibrinogen: mutual inhibition in binding. *Eur J Biochem.* 1984;145:151–156.
34. Murphy-Ullrich JE. The de-adhesive activity of matricellular protein: is intermediate cell adhesion an adaptive state (review)? *J Clin Invest.* 2001;107:785–790.
35. Takagi J, Fujisawa T, Usui T, Aoyama T, Saito Y. A single chain 19-kDa fragment from bovine thrombospondin binds to type V collagen and heparin. *J Biol Chem.* 1993;268:15544–15549.

36. Galvin NJ, Vance PM, Dixit VM, Fink B, Frazier WA. Interaction ofhuman thrombospondin with types I-V collagen: direct binding and electron microscopy. *J Cell Biol.* 1987;104:1413–1422.
37. Marshall GE, Konstas AG, Lee WR. Immunogold fine structural localization of extracellular matrix components in aged human cornea. I. Types I–IV collagen and laminin. *Graefes Arch Clin Exp Ophthalmol.* 1991;229:157–163.
38. Marshall GE, Konstas AG, Lee WR. Immunogold fine structural localization of extracellular matrix components in aged human cornea. II. Collagen types V and VI. *Graefes Arch Clin Exp Ophthalmol.* 1991;229:164–171.
39. Schults-Cherry S, Lawler J, Murphy-Ullrich JE. The type 1 repeats of thrombospondin 1 activate latent transforming growth factor-β. *J Biol Chem.* 1994;269:26783–26788.
40. Armstrong DJ, Hiscott P, Batterbury M, Kaye S. Corneal stromal cells (keratocytes) express thrombospondins 2 and 3 in wound repair phenotype. *Int J Biochem Cell Biol.* 2002;34:588–593.

Neural conversion of ES cells by an inductive activity on human amniotic membrane matrix

Morio Ueno*†‡, Michiru Matsumura*, Kiichi Watanabe*, Takahiro Nakamura†, Fumitaka Osakada*§, Masayo Takahashi§, Hiroshi Kawasaki¶, Shigeru Kinoshita†, and Yoshiki Sasai*‖

*Organogenesis and Neurogenesis Group, RIKEN Center for Developmental Biology, Kobe 650-0047, Japan; †Department of Ophthalmology, Kyoto Prefectural University of Medicine, Kyoto 602-8566, Japan; §Translational Research Center, Kyoto University Hospital, Kyoto 606-8507, Japan; and ¶Department of Molecular and System Neurobiology, Graduate School of Medicine, University of Tokyo, Tokyo 113-0033, Japan

Edited by Igor B. Dawid, National Institutes of Health, Bethesda, MD, and approved May 1, 2006 (received for review January 6, 2006)

Here we report a human-derived material with potent inductive activity that selectively converts ES cells into neural tissues. Both mouse and human ES cells efficiently differentiate into neural precursors when cultured on the matrix components of the human amniotic membrane in serum-free medium [amniotic membrane matrix-based ES cell differentiation (AMED)]. AMED-induced neural tissues have regional characteristics (brainstem) similar to those induced by coculture with mouse PA6 stromal cells [a common method called stromal cell-derived inducing activity (SDIA) culture]. Like the SDIA culture, the AMED system is applicable to the *in vitro* generation of various CNS tissues, including dopaminergic neurons, motor neurons, and retinal pigment epithelium. In contrast to the SDIA method, which uses animal cells, the AMED culture uses a noncellular inductive material derived from an easily available human tissue; therefore, AMED should provide a more suitable and versatile system for generating a variety of neural tissues for clinical applications.

neural differentiation | extracellular matrix | dopaminergic neuron | retinal pigment epithelium | lens

Over the past several years, much progress has been made in the *in vitro* control of neural differentiation of ES cells. Neural conversion of mouse ES (mES) cells can be induced *in vitro* by several methods: retinoic acid (RA) treatment of embryoid bodies (EB) (1, 2), multistep-induction/selection culture (3), serum-free adherent monoculture (4), serum-free suspension culture (5), and feeder cell-dependent induction culture (6–9). Each method has its own advantages and disadvantages, depending on the type of neural cells desired. The different methods induce the differentiation of neural tissues with distinct characteristics, particularly with regard to their regional identities in the CNS (2, 5, 8).

We previously reported a feeder cell-dependent induction method that uses a neuralizing activity located on the surface of PA6 stromal cells [stromal cell-derived inducing activity (SDIA)] (6). SDIA induces neural differentiation from mES cells quickly (<5 days) and efficiently (>90%). In response to exogenous patterning signals such as Sonic hedgehog (Shh), bone morphogenetic protein 4 (BMP4), and RA (8, 10), SDIA-induced neural precursors differentiate into a wide range of neural cells of the CNS that correlate with their positions along the dorsal-ventral and rostral-caudal axes (6, 8). SDIA is also applicable to the generation of medically useful neurons such as dopaminergic neurons and motor neurons not only from mES cells but also from primate ES cells (human and nonhuman) (7, 11, 12). In particular, SDIA-treated ES cells efficiently differentiate into midbrain dopaminergic neurons (≈30% of induced neurons) without the addition of exogenous factors such as Shh (6). This method is in contrast to other methods (e.g., the multiple induction/selection method) (3), which require additional treatment with several inducing factors or gene transfer to efficiently generate dopaminergic neurons. Furthermore, when grafted into the striatum of the 1-methyl-4-phenyl-1,2,3,6-tetrahydropyridine (MPTP)-treated Parkinson's disease model monkey (13), SDIA-induced dopaminergic neurons (from primate ES cells) cause marked improvement in motor function and robustly increase local uptake of the dopamine precursor (Dopa), indicating that the SDIA-induced neurons are functional in the *in vivo* context.

Because of its simple, speedy procedure and good reproducibility, the SDIA method has become one of the standard methods used in human ES (hES) cell-based therapeutic research for neurological diseases such as Parkinson's disease (11, 12, 14–17). However, despite its advantages, the SDIA method has a fundamental practical disadvantage for clinical applications of stem cell therapy: the use of xenogenic (mouse) stromal cells as the source of the inductive signals (6). The involvement of xenogenic cells (and any materials derived from them) presumably increases the risk associated with cocultured tissues in transplantation therapy (18). The hES cell-derived neurons induced with PA6 cells might be contaminated with pathogens or unfavorable antigens originating from the cocultured animal cells. For instance, it has been reported that hES cells cultured on mouse feeder cells express an immunogenic non-human sialic acid on their cell surface (19).

In this study, as an alternative inductive material for neural differentiation of ES cells, we introduce the use of the matrix layers of the human amniotic membrane (hAM). The hAM matrix layers possess intriguing biological activities such as the promotion of wound healing and cell growth (20, 21). Here we show that the hAM matrix layers possess an SDIA-like potent neural-inducing activity. Because the matrix of the hAM is a material widely used in surgical practice (20, 22), it serves as a unique, safe source of neural-inducing factors of human origin, which could circumvent problems associated with the use of xenogenic materials.

Results

Efficient Neural Differentiation of ES Cells on the Denuded hAM. The hAM is composed of an epithelial layer and two matrix layers (the basement membrane and the thick avascular stromal matrix) (23), which underlie the epithelium (illustrated in Fig. 6, which is published as supporting information on the PNAS web site). The matrix layers of hAM (referred to as "denuded hAM"

Conflict of interest statement: No conflicts declared.

This paper was submitted directly (Track II) to the PNAS office.

Abbreviations: mES, mouse ES; hES, human ES; hAM, human amniotic membrane; KSR, knockout serum replacement; AMED, amniotic membrane matrix-based ES cell differentiation; SDIA, stromal cell-derived inducing activity; TH, tyrosine hydroxylase; Shh, Sonic hedgehog; BMP4, bone morphogenetic protein 4; RA, retinoic acid; EB, embryoid bodies.

†Present address: Department of Ophthalmology, National Hospital for Geriatric Medicine, National Center for Geriatrics and Gerontology, Obu 474-8511, Japan.

‖To whom correspondence should be addressed at: Organogenesis and Neurogenesis Group, RIKEN Center for Developmental Biology, 2-2-3 Minatojima-minamimachi, Chuo, Kobe 650-0047, Japan. E-mail: sasaicdb@mub.biglobe.ne.jp.

hereafter) have been shown to possess growth-supporting activity on the stem/progenitor cells of various tissues. For instance, corneal limbal progenitors efficiently grow on denuded hAM and eventually form a well organized epithelial tissue, which is suitable for transplantation (21, 22).

We first tested whether the growth of mES cells was supported on the denuded hAM. A detailed protocol is described in the *Supporting Material and Methods*, which is published as supporting information on the PNAS web site, and illustrated in Fig. 1 *A* and *B* and Fig. 6. Dissociated mES cells formed large colonies when cultured for a week on the gelatin-coated denuded hAM in serum-free differentiation medium [knockout serum replacement (KSR)-based or chemically defined medium; see *Materials and Methods*] without leukemia inhibitory factor (Fig. 1*C*, arrow; the porous filter is seen as the background with halos in this picture). These colonies contained a large proportion of Nestin$^+$ and NCAM$^+$ neural cells (>90%; Fig. 1 *D–F*; day 6). We next examined the generation of neural precursors by using an ES cell line in which GFP cDNA was knocked-in at the locus of the early neural gene *Sox1* [*Sox1-GFP*; line 46C; a gift from A. Smith (University of Edinburgh, Edinburgh)] (24). Strong Sox1-GFP expression first appeared in the ES cells between days 3 and 4 (data not shown), and a substantial cell population became Sox1-GFP$^+$ on day 5 and after (≈90% of the cells on day 5; Fig. 1*G*). Most of the Sox1-GFP$^+$ cells (>90%) coexpressed the neural precursor markers Musashi (Fig. 1*H*) and Nestin (data not shown), indicating a preferential generation of neural precursors from ES cells cultured on hAM. In contrast, treatment with BMP4 (0.5 nM, days 0–5), which is a strong inhibitor of early neural differentiation (6), suppressed the Sox1-GFP expression in ES cells cultured on hAM (Fig. 1*I*; instead, the cells expressed the nonneural epithelial marker E-cadherin; see also Fig. 1 *L* and *M*). RT-PCR analysis showed that ES cells cultured on the denuded hAM did not express the mesodermal marker *Brachyury* or the endodermal markers *AFP* and *Sox17* (Fig. 1*J*, lane 3) in contrast to EB treated with serum (lane 2).

The preferential appearance of neural cells in the culture was unlikely to be caused by the selective adhesion of contaminating neural precursors (ES cell-derived) to the hAM for the following reasons. First, the ES cells used in this study expressed Oct3/4 and Nanog (markers of the undifferentiated state; >95%) in the maintenance culture, whereas no Sox1 expression was observed (data not shown). Second, even 1 or 2 days after plating, ES cells growing on the denuded hAM frequently expressed Oct3/4 (>95%) but not Sox1 (Fig. 1*K*), indicating that the attached cells were undifferentiated.

The Sox1-GFP$^+$ cells on the hAM never expressed the human-specific nuclear antigen (25) ($n > 200$ colonies; Fig. 7*A–C*, which is published as supporting information on the PNAS web site), indicating that these cells were not produced by fusion between the mES cells and contaminating human cells on the denuded hAM. Importantly, both the growth-supporting (data not shown) and neural-inducing (Fig. 1 *M* and *N*; shown by the Sox1-GFP$^+$ populations in FACS analyses) activities of the denuded hAM remained unaffected even after treatment with 0.5% deoxycholate (12 h at 37°C), which thoroughly removed the cellular components from the hAM (see *Supporting Materials and Methods*). This finding indicates that the activities are present in the detergent-resistant extracellular matrices.

Taken together, these observations demonstrate that the hAM matrix provides a potent neural-inducing environment for cocultured ES cells. In the present study, "ES cell differentiation on the denuded hAM" is referred to as amniotic membrane matrix-based ES cell differentiation (AMED) hereafter.

On the hAM matrix, as described above, ES cells grew efficiently and selectively differentiated into Sox1$^+$ neural precursors (at a 90% or higher frequency) in serum-free medium. We next examined whether such highly selective, efficient generation of Sox1$^+$ precursors was seen when other matrix materials were used as a substratum. ES cells were cultured on culture dishes coated with gelatin, collagen IV, laminin, or fibronectin or on dishes with a collagen I gel. In all these cases, the cells grew less robustly than on the hAM matrix, and the efficiency of neural differentiation was substantially lower (60–70%; Fig. 7*F*) even though the same serum-free differentiation medium was

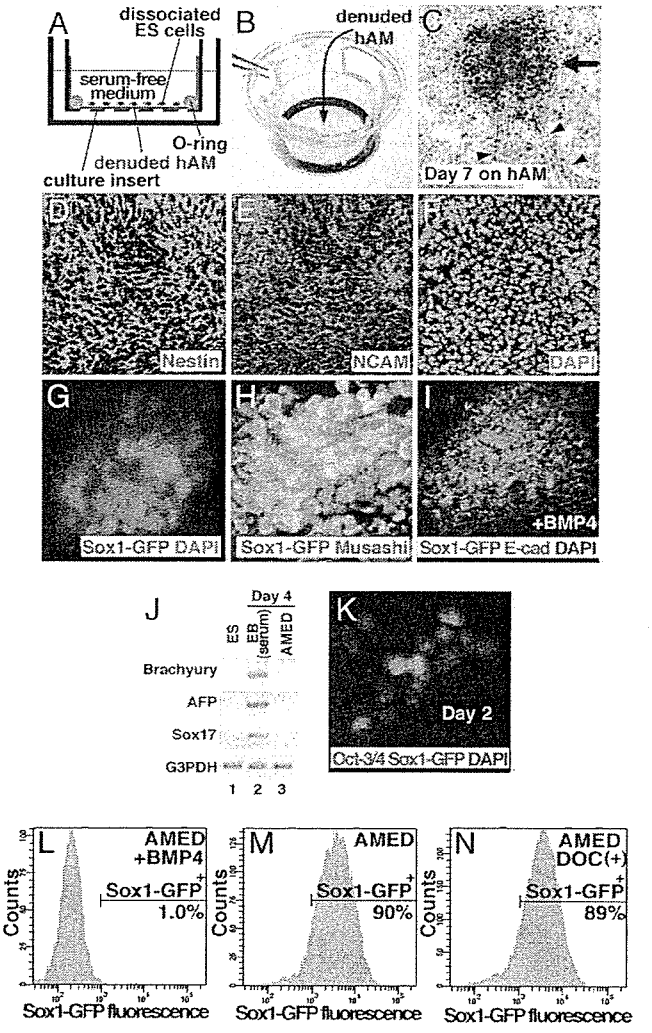

Fig. 1. Efficient induction of neural differentiation from mES cells on the denuded hAM. (*A*) Schematic view of AMED culture. (*B*) Photograph of a culture insert with denuded hAM and O-ring (black). (*C*) Phase-contrast view of a mES cell colony (arrow) cultured on hAM for 1 week. Arrowheads indicate neurites extending from the colony. (*D–F*) Immunostaining of the AMED-treated cells (day 6) with Nestin and NCAM antibodies (*D* and *E*) and nuclear staining with DAPI (*F*). (*G* and *H*) Immunostaining of the AMED-treated cells with neural precursor markers. Sox1-GFP signal (green in *G* and *H*), Musashi (red in *H*, day 7), and DAPI (blue in *G*) are shown. (*I*) Immunostaining analysis of ES cells treated with AMED and BMP4. Sox1-GFP signal (green) was not detected, and most of the cells expressed the nonneural epithelial marker E-cadherin (red), showing that BMP4 inhibited neural differentiation in AMED culture. (*J*) RT-PCR analysis of mesodermal (*Brachyury*) and endodermal (*AFP* and *Sox17*) marker genes. (*K*) Immunostaining of ES cells on hAM for Oct3/4 and Sox1-GFP expression (day 2). Most of the cells expressed Oct3/4 (marker for the undifferentiated state) but not the Sox1-GFP neural precursor marker. (*L–N*) FACS analysis showing efficient neural differentiation (Sox1-GFP expression on day 6) of mES cells cultured on hAM pretreated with deoxycholate (DOC; *N*). (*L*) Negative control for Sox1-GFP expression, ES cells treated with AMED and BMP4 (see also panel *I*). (*M*) Positive control, AMED-treated ES cells.

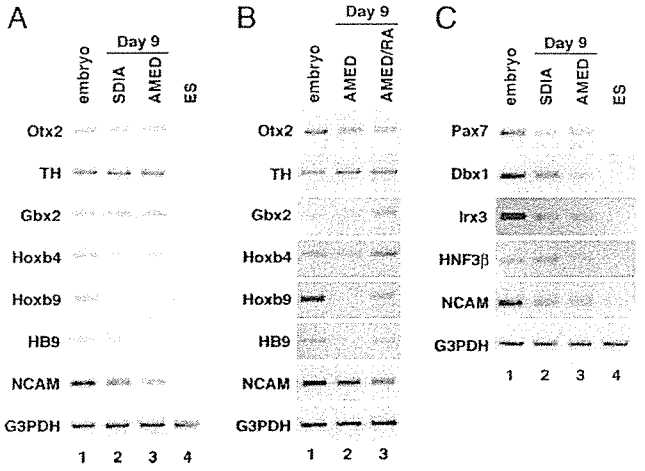

Fig. 2. Regional characterization of AMED-induced neural tissues from mES cells. RT-PCR analysis with the rostral-caudal (*A* and *B*) and dorsal-ventral (*C*) marker genes for CNS tissues. (*A* and *C*) Lane 1, whole embryo (embryonic day 10.5); lane 2, SDIA-treated ES cells (day 9); lane 3, AMED-treated ES cells (day 9); lane 4, undifferentiated ES cells. (*B*) Lane 1, whole embryo (embryonic day 10.5); lane 2, AMED-treated ES cells (day 9); lane 3, AMED- and RA-treated ES cells (day 9).

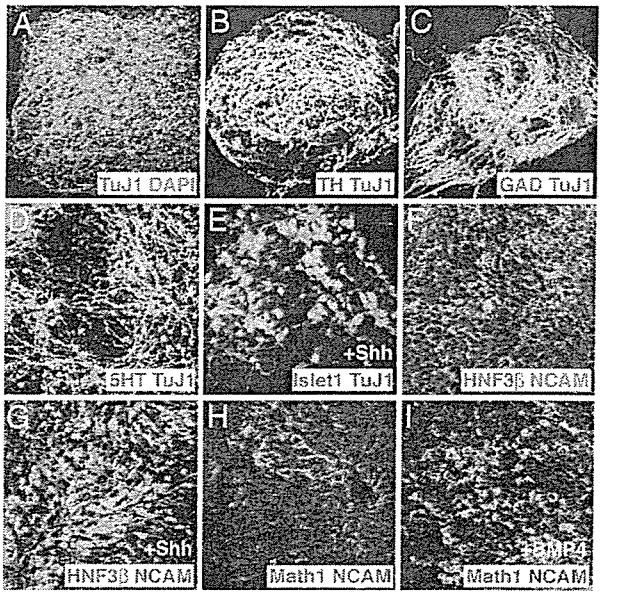

Fig. 3. AMED-treated mES cells generate various types of neural cells including dopaminergic neurons. (*A*) Immunostaining of AMED-treated mES cells with TuJ1 (red) antibody. DAPI, green. (*B–D*) Immunostaining with neurotransmitter-type markers (red) and TuJ1 (green) antibodies (day 13). (*B*) TH for dopamine; (*C*) glutamic acid decarboxylase for GABA; (*D*) 5HT for serotonin. (*E*) Expression of Islet1 in mES cells treated with AMED and Shh (30 nM, days 4–9). (*F* and *G*) Expression of HNF3β in mES cells treated with AMED alone (*F*) and with AMED and Shh (300 nM; *G*). (*H* and *I*) Math1 immunostaining of AMED-treated mES cells with (*I*) or without (*H*) BMP4 treatment (0.5 nM, days 6–10).

used, demonstrating that the hAM matrix has particularly strong supporting activities for the cell growth and neural differentiation of ES cells.

Regional Characterization of the AMED-Induced Neural Tissues. To characterize the nature of the AMED-induced neural tissues, we next performed RT-PCR analyses with regional gene markers. AMED-treated ES cells expressed the forebrain-midbrain markers *Otx2*, *TH* (tyrosine hydroxylase), *Pax2*, and *En2* and the rostral hindbrain marker *Gbx2* at substantial levels (Fig. 2*A*, lane 3 and data not shown). In contrast, little expression was detected for the spinal cord markers *Hoxb4*, *Hoxb9*, and *HB9* (Fig. 2*A*, lane 3).

We recently established another *in vitro* system for neural differentiation of ES cells, namely the SFEB method (serum-free floating culture of EB-like aggregates) (5), which, like AMED, does not use feeder cells as an inducer. SFEB-treated ES cells efficiently generate the rostral-most CNS tissues, particularly $Bf1^+$ telencephalic tissues (15–35%), whereas brainstem tissue differentiation (e.g., dopaminergic neurons) is rare (5). Quantitative analysis using immunostaining indicated that the rostral-most CNS marker Bf1 was rarely expressed in AMED-induced neural cells (<1%; data not shown). Thus, the AMED-induced neural tissues show regional characteristics of the rostral-caudal axis, which are similar to those found in the SDIA culture (mainly brainstem regions) rather than in the SFEB culture (mainly the rostral-most CNS).

The rostral-caudal specification of AMED-induced neural cells could be modified by adding the caudalizing factor RA (Fig. 2*B*). Treatment with RA (0.2 μM, days 4–9) promoted the expression of caudal CNS markers (*Gbx2*, *Hoxb4*, *Hoxb9*, and *HB9*), whereas the forebrain marker *Otx2* was suppressed.

Analyses with dorsal-ventral marker genes showed that the AMED treatment induced both dorsal (*Pax7* and *Dbx1*) and ventral (*Irx3* and *HNF3β*) neural tube markers (Fig. 2*C*, lane 3). Together with the rostral-caudal marker analysis, these findings show that the regional characteristics of the AMED-induced neural tissues are largely similar to those of the SDIA-induced ones (refs. 5 and 8; lane 2 of Fig. 2 *A* and *C*).

AMED-Treated ES Cells Generate a Variety of Neurons Including Dopaminergic Neurons. Immunostaining showed that all of the colonies on day 9 contained a large number of cells that were positive for the postmitotic neuronal marker TuJ1 (62% of total cells; Fig. 3*A*). On day 13, the dopaminergic neuron marker TH was expressed in 39% of the postmitotic neurons (26% of total cells) (Fig. 3*B*). These TH^+ neurons were negative for the noradrenergic marker dopamine β-hydroxylase (data not shown). AMED-treated ES cells contained other neuron types as well, such as GABAergic (glutamic acid decarboxylase-positive; 22% of the neurons; Fig. 3*C*) and serotonergic ($5HT^+$; 1–3% of the neurons; typically rostral hindbrain; Fig. 3*D*) neurons.

Neural precursors induced in the AMED culture could respond to embryologically relevant patterning signals. Treatment with the ventralizing factor Shh (30 nM, days 4–9) efficiently induced the expression of the motor neuron marker Islet1 (32% of the neurons; ventral CNS marker; 5% without Shh treatment) in AMED-cultured ES cells (Fig. 3*E* and data not shown). In addition, the differentiation of $HNF3\beta^+$ $NCAM^+$ cells (floor plate; the ventral-most CNS tissue) was significantly enhanced by Shh treatment at a high dose (3% and 49% of total cells in the absence and presence of 300 nM Shh during days 4–9, respectively; Fig. 3 *F* and *G*). Conversely, treatment with the dorsalizing factor BMP4 (0.5 nM, days 6–10) (8) induced the dorsal CNS marker Math1 (4% of $NCAM^+$ neural cells with BMP4, Fig. 3*I*; <0.1% without BMP4, Fig. 3*H*) but not Islet1 or HNF3β (data not shown).

These observations demonstrate that AMED-induced neural precursors can generate a variety of CNS tissues *in vitro*.

AMED Induces the Differentiation of Neural and Eye Tissues also from hES Cells. Previous studies have shown that the SDIA method is also applicable to neural differentiation of hES cells (11, 12).

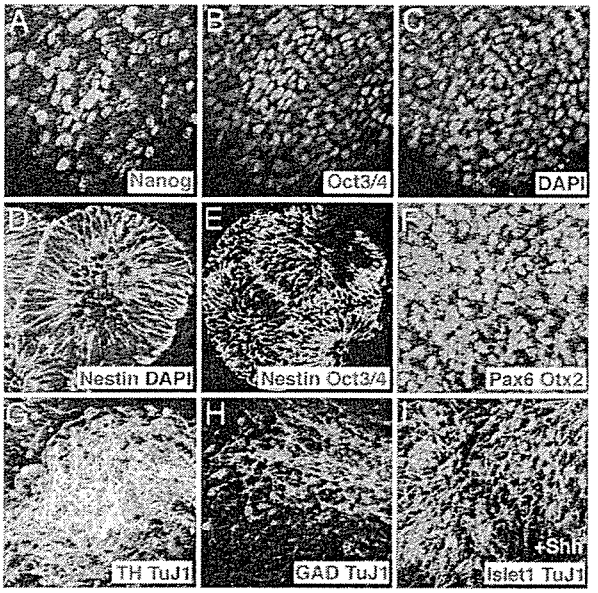

Fig. 4. Neural differentiation of hES cells treated with AMED. (*A–C*) Expression Nanog (red in *A*; Nanog levels were variable as seen in undifferentiated hES cells) and Oct3/4 (green in *B*) in the majority of AMED-treated hES cells on day 2. DAPI (*C*) for nuclear staining. (*D*) Expression of Nestin (green) in AMED-treated hES cells on day 15. DAPI (blue) for nuclear staining. (*E*) Expression of Nestin (green) and Oct3/4 (red) on day 15. (*F*) Mutually exclusive expression of Otx2 (red) and Pax6 (green) in AMED-treated hES cells on day 33. (*G*) Expression of TH (red) in a substantial portion of the TuJ1$^+$ neurons (green) induced from hES cells by AMED (day 40). (*H*) Expression of glutamic acid decarboxylase (red) and TuJ1 (green) on day 42. (*I*) Expression of Islet1 (red) and TuJ1 (green) in AMED/Shh-treated hES cells on day 42.

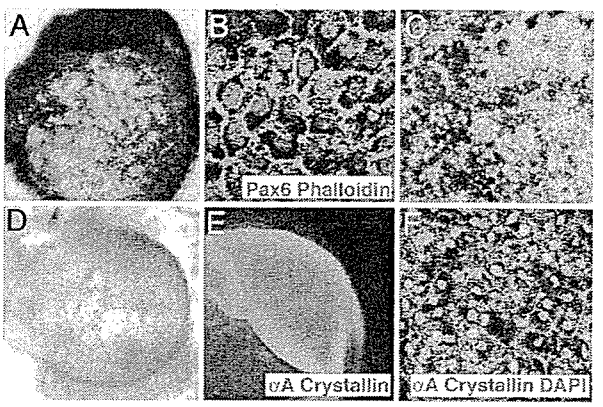

Fig. 5. Differentiation of pigment epithelia and lentoid tissues from AMED-treated hES cells. (*A*) On day 28 and after, pigmented colonies were occasionally found in the culture of hES cells on hAM. (*B*) Phalloidin (red) and anti-Pax6 (green) staining. (*C*) A high-magnification picture of hES cell-derived retinal pigment epithelial cells (pigmented, polygonal) induced in the AMED culture. The pigmented cells were manually isolated from the hAM by a pipette tip and cultured on a culture dish. (*D*) A low-magnification picture of an hES cell-derived lentoid tissue. (*E*) Whole-mount immunostaining with anti-αA-crystallin antibody. (*F*) A high-magnification confocal picture of αA-crystallin (green) and DAPI (red) staining.

Therefore, we next examined whether the AMED treatment promoted neural differentiation also in hES cells. Because hES cells generally do not survive and grow well after complete dissociation, we seeded hES cells in small aggregates (clumps of 5–20 cells) onto the denuded hAM (illustrated in Fig. 8, which is published as supporting information on the PNAS web site). In addition, to enhance cellular attachment to the membrane, the hAM was coated with laminin (see the *Supporting Materials and Methods*). Under these conditions, hES cells reproducibly grew on the hAM and expressed markers for the undifferentiated state (Oct3/4 and Nanog; Fig. 4 *A* and *B*) on day 2. On day 15 of AMED culture, hES cells differentiated into Nestin$^+$ neural precursors at a high frequency (>85% of the cells; Fig. 4*D*). A majority of these Nestin$^+$ neural precursors formed rosette-like clusters. Oct3/4 expression was substantially down-regulated by day 15 and detected only in a small percentage of cells (<5%; they are Nestin$^-$) (Fig. 4*E*; the Oct3/4-positive population disappeared later by day 25). Pax6 expression first appeared on day 15 and was observed in a subpopulation (≈50%) of cells on day 33 (Fig. 4*F*). Expression of the regional marker Otx2 (forebrain and midbrain) was also seen (≈30% of total cells on day 33), whereas the Otx2$^+$ cells were generally negative for Pax6 (Fig. 4*F*). Otx2$^+$/Pax6$^-$ is consistent with the marker expression profile of the midbrain and/or the ventral forebrain, at least in rodent embryos. The telencephalic regional marker Bf1 was not detected in hES cell-derived neural progenitors, at least on and before day 44 (data not shown).

The postmitotic neuronal marker TuJ1 was rarely found on or before day 30 and substantially increased during days 35–40 (Fig. 4*G* and data not shown). On days 40–42, a high percentage of AMED-induced neurons expressed TH (31% of the TuJ1$^+$ neurons; 40% of the total cells were positive for TuJ1; Fig. 4*G*). Expression of the GABAergic neuronal marker glutamic acid decarboxylase was also observed, although less frequently (≈5% of the TuJ1$^+$ neurons; Fig. 4*H*) than TH. The serotonergic neuronal marker (5HT) was detected in <1% neurons (day 44; data not shown). As seen with mES cells (Fig. 3*E*), Shh treatment (300 nM, days 15–42) induced differentiation of Islet1$^+$ neurons in hES cells cultured on the hAM (19% of the TuJ1$^+$ neurons with Shh and <1% without Shh) (Fig. 4*I*).

Our previous studies have shown that SDIA-treated primate ES cells differentiate not only into neural cells but also into eye tissues such as retinal pigment epithelium (7, 26; the retinal pigment epithelium is a CNS tissue derived from the diencephalon during embryogenesis) and lens cells (27). In AMED culture, a number of colonies containing pigmented cells appeared in each well on day 28 (15–40 colonies per well; 200 hES cell clumps were initially seeded per well; Fig. 5*A*). Importantly, these cells were positive for Pax6 and showed actin bundles (Fig. 5*B*; phalloidin staining), consistent with the characteristics of pigment epithelial cells. The pigmented cells could be manually isolated with a pipette tip and grown on a collagen I-coated dish. They exhibited a typical retinal pigment epithelial cell-like morphology (hexagonal cells with a cobblestone-like appearance) (26) under light microscopy (Fig. 5*C*). On day 50 and later, small masses of light-reflecting lentoid tissues were also occasionally found in the culture (Fig. 5*D*). These tissues were αA-crystallin-positive, consistent with the nature of lens cells (Fig. 5 *E* and *F*).

Discussion

Matrix-Associated Neural-Inducing Factors. This study has shown the presence of matrix-associated activities for inducing selective differentiation of neural and sensory tissues from mES and hES cells *in vitro*. Our observations clearly demonstrate that many aspects of the controlled differentiation of AMED-treated ES cells are similar to those of SDIA-treated ones (6–8, 26, 27). Thus, the hAM matrix provides a reasonable human-derived candidate material that can substitute for the mouse-derived feeder layer of PA6 cells as a unique, versatile inducer for neural differentiation in ES cell culture.

At the present, the molecular nature of the inducing activity on the hAM matrix remains to be identified, as does that of the activity on the PA6 cells. A particularly intriguing subject for

future study is to determine how several activities common to the AMED and SDIA methods (e.g., growth support, induction of neural precursors, and differentiation of dopaminergic neurons) are related at the molecular level.

Another important issue, from the mechanistic viewpoint, is to learn which cells are responsible for the accumulation of the AMED activity on the hAM matrix. In the light of their anatomical relationship, one obvious candidate is the amniotic epithelium, which overlies the hAM matrix layers. However, in a preliminary study, we found that neither the amniotic epithelial cells nor their pericellular matrix promotes neural differentiation of cocultured ES cells (our unpublished observations), indicating that the amniotic epithelium, at least by itself, is unlikely to explain the production of the AMED activity.

AMED Culture as a Versatile Method for Generating Neural Cells. The AMED system has several advantages for use in ES cell-based regenerative medicine. (*i*) The AMED culture is remarkably simple; ES cells are plated on the denuded hAM and cultured in a simple serum-free medium. (*ii*) The AMED method uses a human-derived material (denuded hAM) for which the biological safety has been demonstrated for decades in the clinical practices of dermatology and ophthalmology (20, 28, 29). (*iii*) hAM is routinely obtainable from Caesarian sections with proper informed consents. (*iv*) hAM can be easily stored at −80°C for at least for 6 months without losing its AMED activity (see *Supporting Materials and Methods*). Moreover, the neural-inducing activity on the denuded hAM is retained even after lyophilization/rehydration (Fig. 7*G*; lyophilization followed by vacuum packaging and γ-ray irradiation and rehydration in culture medium for 1 hour before use) (30). Therefore, the AMED method could be used to prepare ES cell-derived neurons for cell therapy, regardless of the distance between stem cell laboratories and obstetric clinics.

In future technical improvements of the AMED method, solubilization of the AMED activity from the hAM matrix may be useful because a soluble matrix material could be used to coat culture dishes or even three-dimensional polymer scaffolds (which can support tissue formation from RA-induced neural tissues from hES cells; ref. 31) to further simplify the AMED procedure.

In conclusion, this study demonstrates that the AMED method is potentially useful for producing various neurons for cell therapy from ES cells and that AMED provides a practical solution to avoid the use of xenogenic materials, which are used in the SDIA method.

Materials and Methods

ES Cell Culture. For the maintenance (6), undifferentiated mES cells (EB5 and 46C) were cultured on gelatin-coated dishes at 37°C under 5% CO_2 in Glasgow-MEM (Invitrogen) supplemented with 1% FCS (JRH Biosciences, Lenexa, KS), 10% KSR (Invitrogen), 2 mM glutamine, 0.1 mM nonessential amino acids, 1 mM pyruvate, 0.1 mM 2-mercaptoethanol, and 2,000 units/ml leukemia inhibitory factor (Invitrogen). PA6 cells were maintained in α-MEM with 10% FCS (HyClone) (32).

The hES cells (KhES-1) were a gift from N. Nakatsuji and H. Suemori (Kyoto University) and were used following the hES cell guidelines of the Japanese government. Undifferentiated hES cells were maintained on a feeder layer of mouse embryonic fibroblasts (Invitrogen; inactivated with 10 μg/ml mitomycin C) in DMEM/F12 (Sigma) supplemented with 20% KSR, 2 mM glutamine, 0.1 mM nonessential amino acids (Invitrogen), 5 ng/ml recombinant human bFGF (Upstate), and 0.1 mM 2-mercaptoethanol under 2% CO_2. For passaging, hES cell colonies were detached and recovered *en bloc* from the feeder layer by treating them with 0.25% trypsin and 0.1 mg/ml collagenase IV in PBS containing 20% KSR and 1 mM $CaCl_2$ at 37°C for 7 min, followed by tapping the cultures and flushing them with a pipette. After two volumes of culture medium was added, the detached ES cell clumps were broken into smaller pieces (5–20 cells) by gently pipetting several times. The passages were performed at a 1:4 split ratio. For storage, the ES cell colonies were recovered *en bloc* (without further dissociation) from a 6-cm culture dish, suspended in 1 ml of ice-cold culture medium supplemented with 2 M DMSO, 1 M acetamide, and 3 M polypropylene glycol, and quickly frozen in a 2-ml cryogenic tube (Becton Dickinson Labware) by directly submerging the tube in liquid N_2. The day on which ES cells were seeded on hAM or PA6 cells to start differentiation was defined as day 0.

Preparation of Denuded hAM. With proper informed consent following the tenets of the Declaration of Helsinki, human AMs were obtained under aseptic conditions at the time of Caesarean section. The method of removing the amniotic epithelium from the amniotic membrane has been reported (refs. 21 and 22; see also *Supporting Materials and Methods*). The experiments using the hAM were performed according to the institutional guidelines for human-derived materials.

AMED Culture. The detailed procedures of the AMED culture with mES and hES cells are illustrated in Figs. 6 and 8 and described in the *Supporting Materials and Methods*. For the differentiation medium in this study, we used the KSR-containing G-MEM medium, which was also used in the previous SDIA experiments (6): G-MEM supplemented with 10% KSR, 2 mM glutamine, 1 mM pyruvate, 0.1 mM nonessential amino acids, 0.1 mM 2-mercaptoethanol, 100 units/ml penicillin, and 100 μg/ml streptomycin. In addition to the KSR-based medium used here, we found that chemically defined medium (which does not contain KSR) (33) was suitable for promoting neural differentiation in the AMED culture. The formulation of chemically defined medium is as follows: Iscove's modified Dulbecco's medium/Ham's medium F12 (1:1 ratio) supplemented with glutamine as L-alanyl-L-glutamine or GlutaMAX-I (2 mM; Invitrogen), 5 mg/ml BSA (fraction V), 1× chemically defined lipid concentrate (Invitrogen), 15 μg/ml human apo-transferrin, 0.45 mM monothioglycerol, 7 μg/ml insulin, and 1 unit/ml leukemia inhibitory factor.

Immunostaining, RT-PCR, and FACS Analyses. The antibodies used for immunostaining are listed in the *Supporting Materials and Methods*. Cells were fixed with 4% paraformaldehyde at 4°C for 15 min, and immunostaining was performed as described in refs. 5 and 8 and using secondary antibodies conjugated with FITC, cy3, or cy5. For immunostaining cells in large colonies, confocal microscopy (LSM 510; Zeiss) was used to observe the cells inside the colony with good resolution. The total number of cells was counted by staining nuclei with DAPI. For statistical analyses, 100–200 colonies were examined in each experiment. Experiments were performed at least three times. The values shown in the graphs represent the mean ± SD. RT-PCR was performed with ES cell colonies mechanically detached from the hAM or enzymatically detached from feeder cells as described in refs. 8 and 10. FACS analysis using ES cells with the Sox1-GFP reporter was performed as described in refs. 5 and 24.

We thank H. Niwa (RIKEN Center for Developmental Biology) for the EB5 cells and helpful comments on this work, A. Smith (University of Edinburgh) for the Sox1-GFP ES cells, H. Suemori and N. Nakatsuji (Kyoto University) for providing the hES cell line, H. Kitajima in the Niwa laboratory for kind advice on hES cell expansion and storage, and to the members of the Sasai laboratory for stimulating discussion. This work was supported by grants-in-aid from the Ministry of Education, Culture, Sports, Science, and Technology of Japan (to S.K. and Y.S.), the Kobe Cluster Project (to S.K. and Y.S.), and the Leading Project (to Y.S. and M.T.).

1. Bain, G., Kitchens, D., Yao, M., Huettner, J. E. & Gottlieb, D. I. (1995) *Dev. Biol.* **168,** 342–357.
2. Wichterle, H., Lieberam, I., Porter, J. A. & Jessell, T. M. (2002) *Cell* **110,** 385–397.
3. Lee, S.-H., Lumelsky, N., Studer, L., Auerbach, J. M. & McKay, R. D. (2000) *Nat. Biotechnol.* **18,** 675–679.
4. Ying, Q.-L., Stavridis, M., Griffiths, D., Li, M. & Smith, A. (2003) *Nat. Biotechnol.* **21,** 183–186.
5. Watanabe, K., Kamiya, D., Nishiyama, A., Katayama, T., Nozaki, S., Kawasaki, H., Watanabe, Y., Mizuseki, K. & Sasai, Y. (2005) *Nat. Neurosci.* **8,** 288–296.
6. Kawasaki, H., Mizuseki, K., Nishikawa, S., Kaneko, S., Kuwana, Y., Nakanishi, S., Nishikawa, S.-I. & Sasai, Y. (2000) *Neuron* **28,** 31–40.
7. Kawasaki, H., Suemori, H., Mizuseki, K., Watanabe, K., Urano, F., Ichinose, H., Haruta, M., Takahashi, M., Yoshikawa, K., Nishikawa, S.-I., *et al.* (2002) *Proc. Natl. Acad. Sci. USA* **99,** 1580–1585.
8. Mizuseki, K., Sakamoto, T., Watanabe, K., Muguruma, K., Ikeya, M., Nishiyama, A., Arakawa, A., Suemori, H., Nakatsuji, N., Kawasaki, H., *et al.* (2003) *Proc. Natl. Acad. Sci. USA* **100,** 5828–5833.
9. Barberi, T., Klivenyi, P., Calingasan, N. Y., Lee, H., Kawamata, H., Loonam, K., Perrier, A. L., Bruses, J., Rubio, M. E., Topf, N., *et al.* (2003) *Nat. Biotechnol.* **21,** 1200–1207.
10. Irioka, T., Watanabe, K., Mizusawa, H., Mizuseki, K. & Sasai, Y. (2005) *Dev. Brain. Res.* **154,** 63–70.
11. Buytaert-Hoefen, K. A., Alvarez, E. & Freed, C. R. (2004) *Stem Cells* **22,** 669–674.
12. Brederlau, A., Correia, A. S., Anisimov, S. V., Elmi, M., Roybon, L., Paul, G., Morizane, A., Bergquist, F., Riebe, I., Nanmmark, U., *et al.* (2006) *Stem Cells,* in press.
13. Takagi, Y., Takahashi, J., Saiki, H., Morizane, A., Hayashi, T., Kishi, Y., Fukuda, H., Okamoto, Y., Koyanagi, M., Ideguchi, M., Hayashi, H., *et al.* (2005) *J. Clin. Invest.* **115,** 102–109.
14. Zeng, X., Chen, J., Liu, Y., Luo, Y., Schulz, T. C., Robins, A. J., Rao, M. S. & Freed, W. J. (2004) *Restor. Neurol. Neurosci.* **22,** 421–428.
15. Zeng, X., Cai, J., Chen, J., Luo, Y., You, Z.-B., Fotter, E., Wang, Y., Harvey, B., Miura, T., Backman, C., *et al.* (2004) *Stem Cells* **22,** 925–940.
16. Pomp, O., Brokhman, I., Ben-Dor, I., Reubinoff, B. & Goldstein, R. S. (2005) *Stem Cells* **23,** 923–930.
17. Goldman, S. (2005) *Nat. Biotechnol.* **23,** 862–871.
18. Takeuchi, Y., Magre, S. & Patience, C. (2005) *Rev. Sci. Tech.* **24,** 323–334.
19. Martin, M. J., Muotri, A., Gage, F. & Varki, A. (2005) *Nat. Med.* **11,** 228–232.
20. Trelford, J. D. & Trelford-Sauder, M. (1979) *Am. J. Obstet. Gynecol.* **134,** 833–845.
21. Koizumi, N., Fullwood, N. J., Bairaktaris, G., Inatomi, T., Kinoshita, S. & Quantock, A. J. (2000) *Invest. Ophthalmol. Visual Sci.* **41,** 2506–2513.
22. Koizumi, N., Inatomi, T., Suzuki, T., Sotozono, C. & Kinoshita, S. (2001) *Ophthalmology* **108,** 1569–1574.
23. Bourne, G. L. (1960) *Am. J. Obstet. Gynecol.* **79,** 1070–1073.
24. Aubert, J., Stavridis, M. P., Tweedie, S., O'Reilly, M., Vierlinger, K., Li, M., Ghazal, P., Pratt, T., Mason, J. O., Roy, D., *et al.* (2003) *Proc. Natl. Acad. Sci. USA* **100,** 11836–11841.
25. Uchida, N., Buck, D. W., He, D., Reitsma, M. J., Masek, M., Phan, T. V., Tsukamoto, A. S., Gage, F. H. & Weissman, I. L. (2000) *Proc. Natl. Acad. Sci. USA* **97,** 14720–14725.
26. Haruta, M., Sasai, Y., Kawasaki, H., Amemiya, K., Ooto, S., Kitada, M., Suemori, H., Nakatsuji, N., Ide, C., Honda, Y., *et al.* (2004) *Invest. Ophthalmol. Visual Sci.* **45,** 1020–1025.
27. Ooto, S., Haruta, M., Honda, Y., Kawasaki, H., Sasai, Y. & Takahashi, M. (2003) *Invest. Ophthalmol. Visual Sci.* **44,** 2689–2693.
28. Tsubota, K., Satake, Y., Ohyama, M., Toda, I., Takano, Y., Ono, M., Shinozaki, N. & Shimazaki, J. (1996) *Am. J. Ophthalmol.* **122,** 38–52.
29. Lee, S.-H. & Tseng, S. C. G. (1997) *Am. J. Ophthalmol.* **123,** 303–312.
30. Nakamura, T., Yoshitani, M., Rigby, H., Fullwood, N. J., Ito, W., Inatomi, T., Sotozono, C., Nakamura, T., Shimizu, Y. & Kinoshita, S. (2004) *Invest. Ophthalmol. Visual Sci.* **45,** 93–99.
31. Levenberg, S., Huang, N. F., Lavik, E., Rogers, A. B., Itskovitz-Eldor, J., Langer, R. (2003) *Proc. Natl. Acad. Sci. USA* **100,** 12741–12746.
32. Kawasaki, H., Mizuseki, K. & Sasai, Y. (2001) in *Methods in Molecular Biology* **185,** ed. Turksen, K. (Humana, Totowa, NJ), pp. 217–227.
33. Johansson, B. M. & Wiles, M. V. (1995) *Mol. Cell. Biol.* **15,** 141–151.

Available online at www.sciencedirect.com
SCIENCE DIRECT®
Experimental Eye Research xx (2006) 1–6
EXPERIMENTAL EYE RESEARCH
www.elsevier.com/locate/yexer

Different expression of angiogenesis-related factors between human cultivated corneal and oral epithelial sheets

Eiichi Sekiyama [a,*], Takahiro Nakamura [a,b], Satoshi Kawasaki [a], Hisayo Sogabe [a], Shigeru Kinoshita [a]

[a] *Department of Ophthalmology, Kyoto Prefectural University of Medicine, Graduate School of Medicine, Kawaramachi Hirokoji, Kamigyo-ku, Kyoto 602-0841, Japan*
[b] *Research Center for Regenerative Medicine, Doshisha University, Kyoto, Japan*

Received 15 August 2005; accepted in revised form 25 February 2006

Abstract

We developed a cultivated oral mucosal epithelial sheet (COE) transplantation system to address severe human ocular surface disorders. Unlike the cultivated corneal epithelial sheet (CCE), the COE induces mild superficial peripheral neovascularization although central clarity is maintained. To evaluate the characteristic differences between CCE and COE regarding to angiogenesis, we examined the expression of angiogenesis-related factors in CCE and COE. Using samples of CCE and COE, we immunohistochemically determined protein expression of the angiogenesis related factors: Thrombospondin-1 (TSP-1), pigment epithelium derived factor (PEDF), endostatin, angiostatin, vascular endothelial growth factor (VEGF), Fms-like tyrosine kinase 1 (Flt-1), kinase insert domain receptor (KDR), and basic fibroblast growth factor (bFGF). We used Western blot analysis to confirm the factors that were immunohistochemically different in CCE and COE. The immunohistochemical staining intensity of TSP-1 was higher in CCE than COE and by Western blot analysis the expression of TSP-1 was significantly higher in CCE than COE ($P < 0.05$). PEDF and endostatin stained moderately stronger in CCE than COE. Immunohistochemically there was no obvious difference between CCE and COE with respect to angiostatin, VEGF, Flt-1, KDR, and bFGF. In comparison with CCE, COE showed decreased expression of anti-angiogenic factors particularly TSP-1. This different expression may relate to the superficial peripheral neovascularization encountered after COE transplantation.

Keywords: cultivated epithelial sheet; angiogenesis; thrombospondin-1; ocular surface reconstruction

1. Introduction

To repair severe ocular surface disorders induced by chemical and thermal injuries, Stevens–Johnson syndrome, and ocular cicatricial pemphigoid, we developed a corneolimbal epithelial culture system that uses amniotic membrane (AM) as a carrier (Koizumi et al., 2000a, 2001) and succeeded in the transplantation of cultivated corneal epithelial sheets (CCE). We chose oral mucosa as a source of epithelial cells (Gipson et al., 1986) to establish an autologous transplantation system. We then developed a method for oral epithelial cell cultivation, and succeeded in the transplantation of cultivated oral epithelial sheets (COE) (Nakamura et al., 2004a,b).

Although COE and CCE share many histological (Fig. 1A1–4) and immunohistochemical characteristics and transmission electron microscopy failed to detect marked differences (Nakamura et al., 2004b), the clinical course of patients who received autologous COE transplants differs from that of CCE recipients. Unlike patients transplanted with CCE, most recipients of autologous COE, irrespective of diseases, developed superficial corneal neovascularization measuring 3–4 mm in length from the limbus under the transplanted epithelial sheet (Nakamura et al., 2004b; Nishida

* Corresponding author. Tel.: +81 75 251 5578; fax: +81 75 251 5663.
E-mail address: esekiyam@ophth.kpu-m.ac.jp (E. Sekiyama).

0014-4835/$ - see front matter © 2006 Elsevier Ltd. All rights reserved.
doi:10.1016/j.exer.2006.02.015

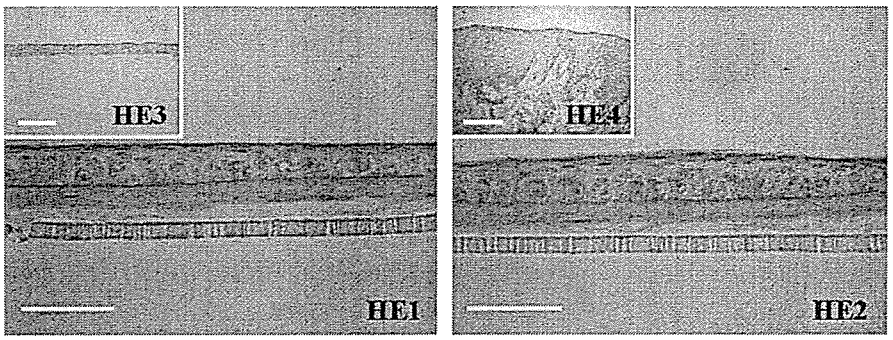

Fig. 1. Representative hematoxylin-eosin staining for CCE (HE1), COE (HE2), normal corneal epithelium (HE3) and normal oral epithelium (HE4).

et al., 2004). Little is known about the pathogenesis of neovascularization after COE transplantation.

We postulated that the mechanism(s) underlying the observed neovascularization was attributable to some characteristics of the oral epithelial cells, and compared CCE and COE with respect to the expression of major angiogenesis-related factors. As our early comparison of the comprehensive gene expression patterns of angiogenesis-related factors in the human corneal- and conjunctival epithelium had shown that only thrombospondin-1 (TSP-1) was significantly up-regulated in the corneal epithelium (Sekiyama et al., 2006), we focused on several factors expressed in the corneal epithelium, including TSP-1. Here we report our first attempt to understand the mechanism(s) of neovascularization after COE transplantation.

2. Materials and methods

2.1. Cultivation of human corneal and oral epithelial cells

Human corneal and oral epithelium, and AM were obtained from donors who provided prior informed consent. Our study followed the tenets of the Declaration of Helsinki and was approved by the Institutional Review Board of Kyoto Prefectural University of Medicine. For epithelial cell culture, five human corneal tissues were obtained from a United States eye bank and five oral mucosal biopsy specimens were donated by healthy volunteers.

For the preparation of human CCE and COE we used a previously reported method (Koizumi et al., 2000b; Nakamura et al., 2003) in which epithelial cells are co-cultured with mitomycin C-inactivated 3T3 fibroblasts. Denuded AM was spread, epithelial basement membrane side up, on the bottom of culture plate inserts (Corning Inc., Corning, NY) and these were placed in dishes containing treated 3T3 fibroblasts. Enzymatically treated corneal limbal or oral epithelial cells were seeded onto the denuded AM prior to 1–2-week submersion in medium. This was followed by 2–3-day exposure to air by lowering the level of the medium (airlifting) to promote epithelial differentiation and barrier function (Koizumi et al., 2000b).

For the controls we used normal human corneal epithelium from corneal buttons of patients undergoing PKP surgery for mild Fuchs corneal dystrophy and superfluous oral tissues from patients who had undergone oral surgery.

2.2. Immunohistochemistry for angiogenesis-related factors

We immunohistochemically investigated the anti-angiogenic factors thrombospondin-1 (TSP-1), pigment epithelium derived factor (PEDF), endostatin, and angiostatin, and the angiogenic factors vascular endothelial growth factor (VEGF), Fms-like tyrosine kinase 1 (Flt-1), kinase insert domain receptor (KDR), and basic fibroblast growth factor (bFGF) in CCE and COE using a modification of our previously described method (Nakamura et al., 2003). Normal human corneal- and oral epithelia were examined for comparison purposes. Briefly, semi-thin (8 μm) cryostat sections were cut from unfixed tissue embedded in optimal cutting temperature compound (Tissue-Tek; Miles Inc., Elkhart, IN). After 5-min fixation in cold acetone the sections were incubated for 15 min with 10% goat serum and 1% bovine serum albumin (Sigma, St. Louis, MO). Then they were incubated at room temperature (RT) for 1 h with the primary antibodies (Table 1) and washed three times for 10 min each in phosphate-buffered saline (PBS). In control experiments we replaced the primary antibody with identical concentrations of the appropriate non-specific normal mouse and rabbit IgG (Dako, Kyoto, Japan). In the negative controls we replaced the primary antibody with the appropriate non-immune IgG.

After incubation with the primary antibody, the sections were washed with PBS containing 0.15% TritonX-100 (PBST) and incubated for 1 h at RT with the appropriate

Table 1
Primary antibodies used for immunohistochemistry

Antibodies	Category	Dilution	Source
TSP-1	Mouse monoclonal	×100	Sigma (St. Louis, MO)
PEDF	Mouse monoclonal	×100	Chemicon (Temecula, CA)
Endostatin	Mouse monoclonal	×100	Upstate (Lake Placid, NY)
Angiostatin	Rabbit monoclonal	×50	Oncogene (San Diego, CA)
VEGF	Mouse monoclonal	×100	Upstate (Lake Placid, NY)
Flt-1	Mouse monoclonal	×30	Chemicon (Temecula, CA)
KDR	Mouse monoclonal	×40	Abcam (Cambridge, MA)
bFGF	Mouse monoclonal	×100	Upstate (Lake Placid, NY)

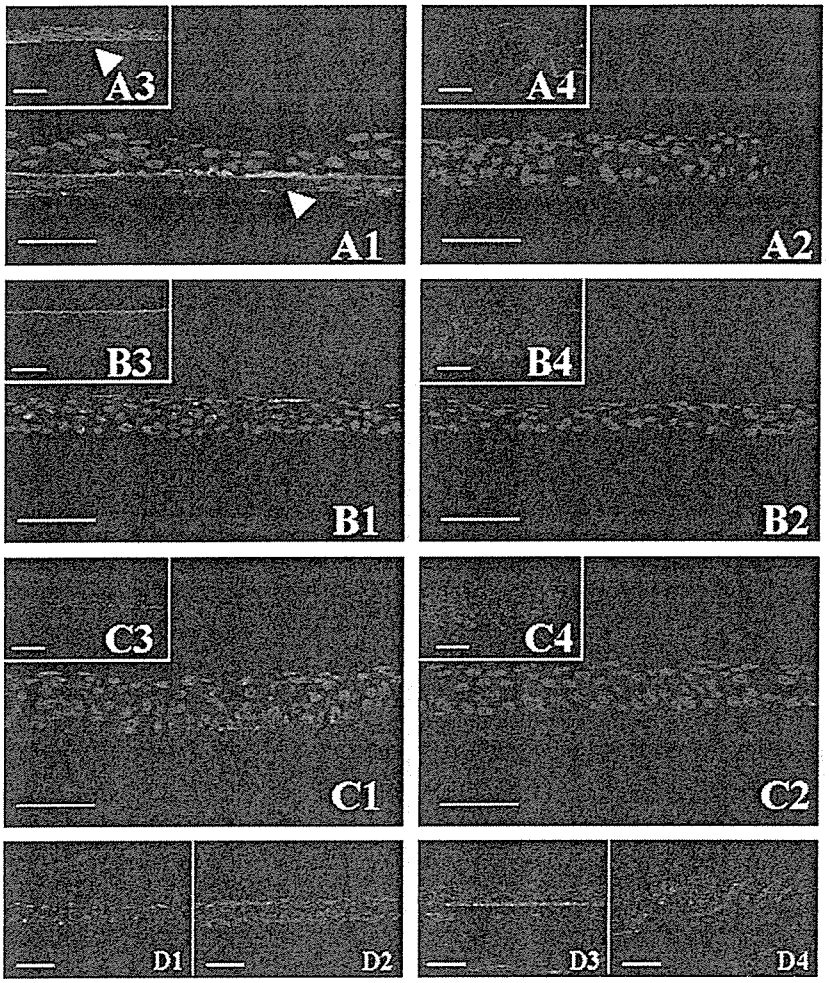

Fig. 2. Representative immunohistochemical staining for anti-angiogenic factors TSP-1 (A), PEDF (B), endostatin (C) and angiostatin (D) in CCE (1), COE (2), normal corneal epithelium (3) and normal oral epithelium (4). TSP-1 was expressed in the basal layer of CCE (A1, arrow) and normal corneal epithelium (A3, arrow), and much less strongly in COE (A2) and normal oral epithelium (A4). PEDF was expressed slightly in CCE (B1), barely in COE (B2), and in the superficial and middle layer of normal corneal epithelium (B3). It was not expressed in normal oral epithelium (B4). Endostatin was expressed in CCE (C1) and normal corneal epithelium (C3), and barely expressed in COE (C2) and normal oral epithelium (C4). Angiostatin was expressed in all examined epithelia (D1–4). Scale bars: 1 and 2: 50 μm; 3: 100 μm; 4: 200 μm.

secondary antibodies, FITC-conjugated anti-mouse, or rabbit IgG antibodies (Molecular Probes Inc., Eugene, OR). After several washes with PBS, the sections were coverslipped using antifade mounting medium containing propidium iodide (Vectashield; Vector, Burlingame, CA) and examined under a confocal microscope (Fluoview; Olympus, Tokyo, Japan).

2.3. Western blot analysis

In our immunohistochemical studies, each fluorescent image was qualitatively and independently scored (3: intense; 2: moderate; 1: faint; 0: negligible) by four examiners in a masked fashion. We took the average of the points scored by the examiners for each sample and assessed statistical significance with the Mann–Whitney *U*-test. Since there was a significant difference between the scores assigned for CCE and COE, we performed Western blots for TSP-1 analysis. CCE and COE were lysed with PBS with 0.1% SDS and 0.1% Triton. For the positive control we used normal human corneal epithelium. The protein content of lysates was determined by bicinchoninic acid (BCA) protein assay (Pierce, Rockford, IL). Aliquots of the lysates were diluted 1:1 with sample buffer (Owl Scientific Inc., Woburn, MA) and heated for 5 min at 95 °C. Equal quantities of protein from lysates (10 μg in 12.5% gel) were subjected to 1 h SDS–PAGE at RT. The separated proteins were then transferred to polyvinylidene difluoride membranes (Immuno-Blot™ PVDF Membrane; Bio-Rad, Hercules, CA) for 12 h at 4 °C and after transfer, the blots were incubated for 30 min in blocking solution (Perfect-Block, MoBi Tec, Goettingen, Germany), washed three times for 10 min each with washing buffer (Tris-buffered saline with 0.1% Tween-20) and then probed for 1 h with anti-TSP-1 (Santa Cruz Biotechnology, Santa Cruz, CA) diluted with washing buffer. After

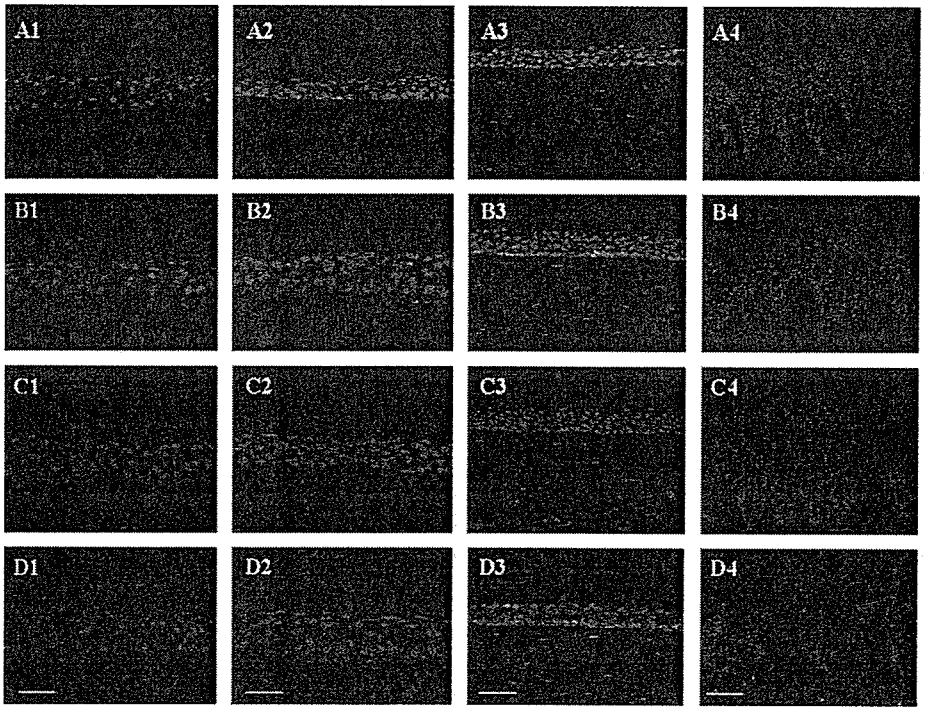

Fig. 3. Representative immunohistochemical staining for angiogenic factors VEGF (A), Flt-1 (B), KDR (C), bFGF (D) in CCE (1), COE (2), normal corneal epithelium (3) and normal oral epithelium (4). VEGF was expressed in the entire layer of CCE (A1), and COE (A2), in the entire, especially the superficial, layer of normal corneal epithelium (A3), and in the middle layer of normal oral epithelium (A4). Flt-1 was weakly expressed in all examined epithelia (B1–4). KDR was not expressed in any examined epithelia (C1–4). Basic FGF was not expressed in CCE and COE (D1 and 2) but was expressed in the basal layer of normal corneal epithelium (D3, arrow) and the middle layer of normal oral epithelium (D4). Scale bars: 1 and 2: 50 μm; 3: 100 μm; 4: 200 μm.

incubation with the primary antibody, the blots were washed three times for 10 min each with washing buffer and then probed with the biotinylated alkaline phosphatase-conjugated secondary antibody (Bio-Rad) diluted with washing buffer. The blots were subsequently developed using the Immune-Blot detection kit (Bio-Rad) and the membranes were then scanned into a computer where band density was digitized using NIH image software.

3. Results

3.1. Immunohistochemistry of human corneal and oral epithelial culture sheets

Cryopreserved CCE and COE were examined. Negative-control sections, incubated with normal mouse and rabbit IgG in the absence of primary antibody, exhibited no discernible specific immunoreactivity over the entire region.

While we detected TSP-1 beneath the cultivated corneal epithelial cells (Fig. 2A1) and normal corneal epithelium (Fig. 2A3), its expression in COE (Fig. 2A2) and normal oral epithelium was minimal or absent (Fig. 2A4). PEDF, slightly expressed in CCE (Fig. 2B1) and barely expressed in COE (Fig. 2B2), was expressed in the superficial and middle layer of normal corneal epithelium (Fig. 2B3) but not in normal oral epithelium (Fig. 2B4). Endostatin, expressed in the entire layer of CCE (Fig. 2C1), in normal corneal epithelium (Fig. 2C3), and in the middle layer of normal oral epithelium (Fig. 2C4), was not expressed in COE (Fig. 2C2). There was no obvious difference between CCE and COE in the expression of angiostatin (Fig. 2D1–4). The staining intensity for TSP-1 was clearly higher in CCE than COE and the staining intensity for PEDF and endostatin was moderately higher in CCE than COE.

VEGF and Flt-1 were expressed in all epithelia examined and there was no significant difference between CCE and COE (Fig. 3A1–4 and B1–4). None of the examined epithelia expressed KDR (Fig. 3C1–4). Basic FGF was not expressed in CCE or COE, but was expressed in the basal layer of normal corneal epithelium and in the middle layer of normal oral epithelium (Fig. 3D1–4). A summary of our immunohistochemical results is provided in Table 2.

3.2. Western blot analysis for TSP-1

We performed Western blots for TSP-1 to determine the protein expression level in CCE and COE. In the presence of TSP-1 antibody there clearly was a single protein band (Fig. 4A); its density was analyzed with NIH image software. As shown in Fig. 4B, TSP-1 was expressed more highly in CCE than COE ($P < 0.05$ by the Mann–Whitney U-test).

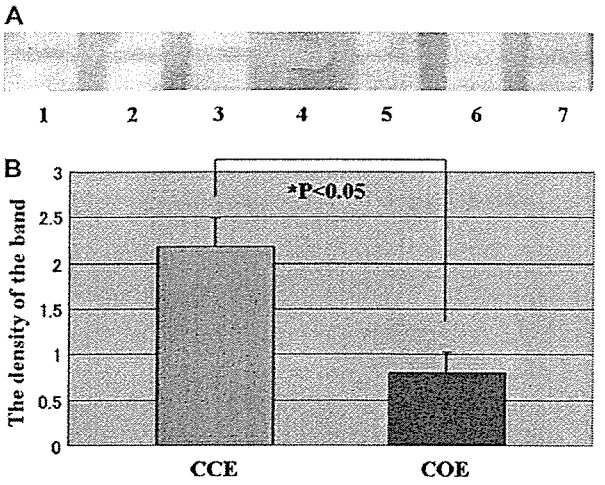

Fig. 4. (A) For TSP-1, Western blots of extracts from CCE (lanes 1, 2, 3) and COE (lanes 5, 6, 7) are shown. Lane 4 shows the molecular weight marker (150 kDa). (B) Average band density analyzed with NIH image software. The density of the CCE is significantly higher than in the COE ($P < 0.05$). The results were statistically compared using the Mann–Whitney U-test. ($n = 3$; mean ± SD: 0.12, mean ± SD: 0.09).

4. Discussion

Immunohistochemically, the staining intensity for TSP-1, the major anti-angiogenic factor contributing to corneal avascularity (Tuszynski and Nicosia, 1996; Castle et al., 1997; Iruela-Arispe et al., 1999; Cursiefen et al., 2004), was higher in CCE than COE and although Western blot analysis detected TSP-1 in both CCE and COE, it was more highly expressed in CCE ($P < 0.05$). Previous studies in TSP-1 knockout mice revealed that their sutured corneas exhibited significantly higher angiogenesis compared with the background strains (Cursiefen et al., 2004). This observation led to the suggestion that TSP-1 plays a role in the suppression of inflammation-induced corneal angiogenesis and that the corneal angiogenic privilege is actively maintained. As the neovascularization we observed in the human recipients of COE transplants may be comparable to the suture-induced angiogenesis in mice, we suggest that the murine findings support our hypothesis that the inflammation-induced corneal neovascularization in the recipients of COE is attributable to the low expression of TSP-1 in these tissues.

Table 2
Immunohistochemical results for each angiogenic factor in each of the examined samples

Factor	NCE	NOE	CCE	COE
TSP-1	2+	0.5+	2+	0.5+
PEDF	2+	–	+	–
Endostatin	+	0.5+	+	–
Angiostatin	+	+	+	+
VEGF	+	+	+	+
Flt-1	+	+	+	+
KDR	–	–	–	–
bFGF	+	+	–	–

NCE, normal corneal epithelium; NOE, normal oral epithelium. 2+, intense expression; +, moderate expression; 0.5+, faint expression; –, negligible expression. Staining intensities for TSP-1, PEDF and endostatin were higher in CCE than COE, and the intensity of TSP-1 staining was particularly high in CCE.

Immunohistochemistry detected TSP-1 expression not only beneath the basal epithelial cells of CCE, but also in AM (Fig. 1B3). As TSP-1 is secreted by fibroblasts, vascular endothelial cells, and smooth muscle cells (Mumby et al., 1984), the TSP-1 we detected could have been secreted by fibroblasts in the stroma of AM. To rule out the possibility that the different expression of TSP-1 in CCE and COE was due to variations in the AM, we performed identical experiments using γ-ray-sterilized AM (Nakamura et al., 2004c) which rendered the fibroblasts not viable. As was the case in denuded AM, TSP-1 was expressed beneath the basal epithelial cells of CCE grown on sterilized AM (data not shown). This observation confirms that the TSP-1 we observed was secreted not by fibroblasts in the stroma of AM, but by epithelial cells, particularly corneal epithelial cells.

Immunohistochemically, the staining intensity for PEDF was slightly higher in CCE than COE. Although we did not perform quantitative PEDF analysis here, studies are underway to examine whether PEDF is an inhibitor of neovascularization under COE. PEDF is one of the major anti-angiogenic factors essential for corneal avascularity (Murthy et al., 2003; Shao et al., 2004) and it more effectively inhibits endothelial cell migration than TSP-1, endostatin, and angiostatin (Dawson et al., 1999).

Endostatin, a potent angiogenesis inhibitor and contributor to corneal avascularity (Chang et al., 2001; Lin et al., 2001; Morbidelli et al., 2003), is expressed in CCE, but not in COE. We are in the process of examining the possible inhibitory effects of endostatin on neovascularization under COE. Ma et al. (2004), who examined the in vitro anti-angiogenic activities of human corneal epithelial cells cultivated on human AM, found that endostatin was a major factor contributing to the anti-angiogenic activity exhibited by human corneal limbal epithelial cells. When they quantitated anti-angiogenic factors in culture supernatants, they found that only the endostatin level was increased. We postulate that TSP-1, bound to the extracellular matrix (Galvin et al., 1987; Krutzsch et al., 1999; Panetti et al., 1999) did not dissolve into the supernatant, and/or that different culture conditions such as the concentration of EGF (Soula-Rothhut et al., 2004) and/or glucose (Wang et al., 2004) affect the expression of TSP-1.

Immunohistochemically, VEGF and Flt-1 were expressed in all the samples we examined; KDR was not expressed in any of our samples. This indicates that neither VEGF nor Flt-1 is a major factor in neovascularization after COE transplantation.

While normal corneal and oral epithelium expressed bFGF, CCE and COE did not. In vivo, bFGF binds to constituents of the extracellular matrix such as heparin sulfate (Van Setten et al., 1995; Okada-Ban et al., 2000). However, in vitro, the constituents of the epithelial extracellular matrix, particularly in the basement membrane, are different. While we did not examine whether bFGF was expressed in transplanted epithelial sheets, we postulate that its expression increases

post-transplantation due to factors such as inflammation and mechanical stress.

Although our earlier histological and electron-microscopic studies disclosed that COE and CCE manifest similar characteristics (Nakamura et al., 2004b), the current study revealed that they differ with respect to the expression of anti-angiogenic factors, particularly TSP-1. We postulate that this difference may be one of the causes of superficial peripheral neovascularization observed after COE transplantation. Further investigations regarding the inhibitory effects of TSP-1 on this neovascularization are needed.

Acknowledgement

The authors thank Kenichi Endo for assisting with Western blot analysis.

References

Castle, V.P., Dixit, V.M., Polverini, P.J., 1997. Thrombospondin-1 suppresses tumorigenesis and angiogenesis in serum- and anchorage-independent NIH 3T3 cells. Lab. Invest. 77 (1), 51–61.

Chang, J.H., Gabison, E.E., Kato, T., Azar, D.T., 2001. Corneal neovascularization. Curr. Opin. Ophthalmol. 12 (4), 242–249.

Cursiefen, C., Masli, S., Ng, T.F., 2004. Roles of thrombospondin-1 and -2 in regulating corneal and iris angiogenesis. Invest. Ophthalmol. Vis. Sci. 45 (4), 1117–1124.

Dawson, D.W., Volpert, O.V., Gillis, P., et al., 1999. Pigment epithelium-derived factor: a potent inhibitor of angiogenesis. Science 285 (5425), 245–248.

Galvin, N.J., Vance, P.M., Dixit, V.M., Fink, B., Frazier, W.A., 1987. Interaction of human thrombospondin with types I-V collagen: direct binding and electron microscopy. J. Cell Biol. 104 (5), 1413–1422.

Gipson, I.K., Geggel, H.S., Spurr-Michaud, S.J., 1986. Transplantation of oral mucosal epithelium to rabbit ocular surface wounds in vivo. Arch. Ophthalmol. 104, 1529–1533.

Iruela-Arispe, M.L., Lombardo, M., Krutzsch, H.C., Lawler, J., Roberts, D.D., 1999. Inhibition of angiogenesis by thrombospondin-1 is mediated by 2 independent regions within the type 1 repeats. Circulation 100 (13), 1423–1431.

Koizumi, N., Inatomi, T., Quantock, A.J., Fullwood, N.J., Dota, A., Kinoshita, S., 2000a. Amniotic membrane as a substrate for cultivating limbal corneal epithelial cells for autologous transplantation in rabbits. Cornea 19, 65–71.

Koizumi, N., Fullwood, N.J., Bairaktaris, G., Inatomi, T., Kinoshita, S., Quantock, A.J., 2000b. Cultivation of corneal epithelial cells on intact and denuded human amniotic membrane. Invest. Ophthalmol. Vis. Sci. 41, 2506–2513.

Koizumi, N., Inatomi, T., Suzuki, T., Sotozono, C., Kinoshita, S., 2001. Cultivated corneal epithelial stem cell transplantation in ocular surface disorders. Ophthalmology 108, 1569–1574.

Krutzsch, H.C., Choe, B.J., Sipes, J.M., Guo, N., Roberts, D.D., 1999. Identification of an alpha (3) beta (1) integrin recognition sequence in thrombospondin-1. J. Biol. Chem. 274 (34), 24080–24086.

Lin, H.C., Chang, J.H., Jain, S., et al., 2001. Matrilysin cleavage of corneal collagen type XVIII NC1 domain and generation of a 28-kDa fragment. Invest. Ophthalmol. Vis. Sci. 42, 2517–2524.

Ma, D.H., Yao, J.Y., Yeh, L.K., et al., 2004. In vitro antiangiogenic activity in ex vivo expanded human limbocorneal epithelial cells cultivated on human amniotic membrane. Invest. Ophthalmol. Vis. Sci. 45 (8), 2586–2595.

Morbidelli, L., Donnini, S., Chillemi, F., Giachetti, A., Ziche, M., 2003. Angiosuppressive and angiostimulatory effects exerted by synthetic partial sequences of endostatin. Clin. Cancer Res. 9 (14), 5358–5369.

Mumby, S.M., Abbott-Brown, D., Raugi, G.J., Bornstein, P., 1984. Regulation of thrombospondin secretion by cells in culture. J. Cell Physiol. 120 (3), 280–288.

Murthy, R.C., McFarland, T.J., Yoken, J., et al., 2003. Corneal transduction to inhibit angiogenesis and graft failure. Invest. Ophthalmol. Vis. Sci. 44 (5), 1837–1842.

Nakamura, T., Endo, K., Cooper, L.J., et al., 2003. The successful culture and autologous transplantation of rabbit oral mucosal epithelial cells on amniotic membrane. Invest. Ophthalmol. Vis Sci. 44, 106–116.

Nakamura, T., Inatomi, T., Sotozono, C., Koizumi, N., Kinoshita, S., 2004a. Successful primary culture and autologous transplantation of corneal limbal epithelial cells from minimal biopsy for unilateral severe ocular surface disease. Acta Ophthalmol. Scand. 82 (4), 468–471.

Nakamura, T., Inatomi, T., Sotozono, C., Amemiya, T., Kanamura, N., Kinoshita, S., 2004b. Transplantation of cultivated autologous oral mucosal epithelial cells in patients with severe ocular surface disorders. Br. J. Ophthalmol. 88 (10), 1280–1284.

Nakamura, T., Yoshitani, M., Rigby, H., et al., 2004c. Sterilized, freeze-dried amniotic membrane: a useful substrate for ocular surface reconstruction. Invest. Ophthalmol. Vis. Sci. 45 (1), 93–99.

Nishida, K., Yamato, M., Hayashida, Y., et al., 2004. Corneal reconstruction with tissue-engineered cell sheets composed of autologous oral mucosal epithelium. N. Engl. J. Med. 351 (12), 1187–1196.

Okada-Ban, M., Thiery, J.P., Jouanneau, J., 2000. Fibroblast growth factor-2 [Review]. Int. J. Biochem. Cell. Biol. 32 (3), 263–267.

Panetti, T.S., Kudryk, B.J., Mosher, D.F., 1999. Interaction of recombinant procollagen and properdin modules of thrombospondin-1 with heparin and fibrinogen/fibrin. J. Biol. Chem. 274 (1), 430–437.

Sekiyama, E., Nakamura, T., Cooper, L.J., Kawasaki, S., Hamuro, J., Fullwood, N.J., Kinoshita, S., 2006. Unique distribution of thrombospondin-1 in human ocular surface epithelium. Invest. Ophthalmol. Vis. Sci. 47 (4), 1352–1358.

Shao, C., Sima, J., Zhang, S.X., et al., 2004. Suppression of corneal neovascularization by PEDF release from human amniotic membranes. Invest. Ophthalmol. Vis. Sci. 45 (6), 1758–1762.

Soula-Rothhut, M., Coissard, C., Sartelet, H., et al., 2004. The tumor suppressor PTEN inhibits EGF-induced TSP-1 and TIMP-1 expression in FTC-133 thyroid carcinoma cells. Exp. Cell. Res. 304 (1), 187–201.

Tuszynski, G.P., Nicosia, R.F., 1996. The role of thrombospondin-1 in tumor progression and angiogenesis. Bioessays 18 (1), 71–76.

Van Setten, G.B., Fagerholm, P., Cuevas-Sanchez, P., 1995. Presence of basic fibroblast growth factor in corneal epithelium. Ophthalm. Res. 27 (6), 317–321.

Wang, S., Skorczewski, J., Feng, X., et al., 2004. Glucose up-regulates thrombospondin 1 gene transcription and transforming growth factor-beta activity through antagonism of cGMP-dependent protein kinase repression via upstream stimulatory factor 2. J. Biol. Chem. 279 (33), 34311–34322.

Establishment of a Cultivated Human Conjunctival Epithelium as an Alternative Tissue Source for Autologous Corneal Epithelial Transplantation

Hidetoshi Tanioka,[1] *Satoshi Kawasaki,*[1] *Kenta Yamasaki,*[1] *Leonard P. K. Ang,*[1,2] *Noriko Koizumi,*[2] *Takahiro Nakamura,*[1] *Norihiko Yokoi,*[1] *Aoi Komuro,*[1] *Tsutomu Inatomi,*[1] *and Shigeru Kinoshita*[1]

Purpose. The corneal epithelium is essential for maintaining corneal transparency, and efforts have been made to develop improved techniques for corneal epithelial transplantation in patients with total limbal failure. We evaluated the suitability of transplanted cultivated human conjunctival epithelium (HCjE) as a corneal epithelium replacement in rabbits with total corneal and limbal deficiency.

Methods. HCjE cells, cultivated on human amniotic membrane (AM) to confluence and exposed to an air–liquid interface (air-lifted), were transplanted onto denuded rabbit corneas and monitored for 2 weeks. The cultivated HCjE sheet and the engrafted epithelium were analyzed by immunohistochemistry and transmission electron microscopy (TEM).

Results. The transplanted HCjE remained transparent, smooth, and without epithelial defects during the follow-up period. Both the cultivated HCjE cells and the engrafted epithelium manifested five to six layers of stratified squamous epithelium similar in morphology to normal corneal epithelium. The basal cells expressed the putative stem cell markers (ABCG2 and P63) and hemidesmosome and desmosome component proteins. The cytokeratins (CK4, CK13, CK3, and CK12) and MUC4 were found in the engrafted epithelium. However, MUC5AC was not expressed. The results indicate that HCjE cultivated on AM has the potential to be used as an alternative corneal epithelium.

Conclusions. The transplantation of cultivated HCjE sheets is a promising technique for the treatment of eyes with limbal failure. (*Invest Ophthalmol Vis Sci.* 2006;47:3820–3827) DOI: 10.1167/iovs.06-0293

The ocular surface is covered by at least two different types of epithelia: corneal and conjunctival.[1–4] These two epithelial tissues are indispensable in keeping homeostasis of the eye by expressing various specific genes such as cytokeratin 3/12 or secretory mucin[2,5,6] and is necessary for ocular surface homeostasis. In patients with severe ocular surface disorders such as Stevens-Johnson syndrome (SJS), ocular cicatricial pemphigoid (OCP), and chemical injuries, the corneal epithelium may be destroyed and replaced by conjunctival epithelium (conjunctivalization). The ocular surface is often inflamed, vascularized, opacified, and keratinized, and vision is severely compromised.

Cultivated corneal stem cells[7–12] and oral epithelia[13–15] transplantations are a newly developed surgical strategy in which to treat such pathologic conditions. Although these treatments were reported to be effective in applying regenerative medicine, several problems remain. For example, tissue transplantation from allogeneic donors carries the risk of rejection and may require postoperative immunosuppressive therapy that can induce severe systemic and local side effects. The longevity of cultivated corneal and oral mucosal epithelium remains to be investigated.

In addition to corneal and oral mucosal epithelium, conjunctival epithelium is a third epithelial cell source that can be cultivated to be transplanted for ocular surface reconstruction. Among all stratified epithelial tissues in the body, these cells are most akin biologically to corneal epithelial cells. Therefore, conjunctival epithelial cells transplanted onto the corneal surface may serve some of the functions of corneal epithelial cells. As the transplantation of cultivated human conjunctival epithelial cells (HCjE) succeeded in reconstructing the conjunctiva of patients with various ocular surface conditions, e.g., pterygium,[16–20] we postulated that cultivated HCjE sheets could be transplanted onto the corneal surface.

To test our hypothesis, we cultured HCjE on human amniotic membrane (AM) and transplanted them onto denuded rabbit corneas. The transplanted HCjE were well-maintained and remained clear and smooth during the postoperative period. Histologic and immunohistochemical analyses revealed that the engrafted epithelium shared the morphology and characteristics of corneal epithelium, suggesting that cultivated HCjE may represent a viable alternative to replace damaged corneal epithelium.

Methods

Human Subjects

This research was approved by the Committee for Ethical Issues on Human Research of Kyoto Prefectural University of Medicine and adhered to the tenets of the Declaration of Helsinki. Normal conjunctival tissues were obtained from patients with conjunctivochalasis. Human AM was harvested at the time of Cesarean section and processed by previously reported methods.[21] The procedures were carefully explained to all donors, and their prior informed consent for use of their tissue was obtained.

From the [1]Department of Ophthalmology, Kyoto Prefectural University of Medicine, Kyoto, Japan; and the [2]Singapore National Eye Center, Singapore.

Supported by Grant-in-Aid 16390502 for scientific research from the Ministry of Education, Science, Culture, and Sports of Japan.

Submitted for publication March 18, 2006; revised April 27, 2006; accepted July 14, 2006.

Disclosure: **H. Tanioka**, None; **S. Kawasaki**, None; **K. Yamasaki**, None; **L.P.K. Ang**, None; **N. Koizumi**, None; **T. Nakamura**, None; **N. Yokoi**, None; **A. Komuro**, None; **T. Inatomi**, None; **S. Kinoshita**, None

The publication costs of this article were defrayed in part by page charge payment. This article must therefore be marked "*advertisement*" in accordance with 18 U.S.C. §1734 solely to indicate this fact.

Corresponding author: Hidetoshi Tanioka, Department of Ophthalmology, Kyoto Prefectural University of Medicine, 465 Kajii-cho, Hirokoji-agaru, Kawaramachi-dori, Kamigyo-ku, Kyoto, 602-0841, Japan: htanioka@eye.ophth.kpu-m.ac.jp.

Investigative Ophthalmology & Visual Science, September 2006, Vol. 47, No. 9

Primary Culture of HCjE Cells

The cells were cultured according to a slightly modified, previously reported system.[22] Briefly, denuded human AM was placed on a porous support membrane (Millipore Corp., Bedford, MA) with the epithelial basement membrane side up. The membrane was then introduced into wells of a six-well culture plate containing mitomycin-treated feeder cells (NIH 3T3; American Type Culture Collection, Manassas, VA) to achieve a dual-chamber culture. After a 1-hr incubation with 1.2 IU dispase (Roche, Tokyo, Japan), the human conjunctival epithelium (the area of this conjunctival source was ~15 mm^2) was removed from the underlying stroma by mechanical scraping and further dissociated by digestion with 0.1% Trypsin-EDTA. The HCjE cells were then seeded on the upper chamber of the culture system and grown according to a three-step culture regimen. Until they reached confluence (6–8 days), the cells were grown in low-calcium medium (Defined Keratinocyte-SFM; Invitrogen, Tokyo, Japan) containing 2% FBS. After reaching confluence, they were grown for 7 days in high-calcium medium (mixture of Defined Keratinocyte-SFM and DMEM/F12/10% FBS at a ratio of 1:1) to promote differentiation. They were then exposed to air by decreasing the volume of the medium (air-lifting) over the course of 1 week to promote epithelial integrity. All cultures were incubated at 37°C in a 5% CO_2-95% air incubator. The medium was changed every day or every other day.

Conjunctival Epithelium Transplantation onto Rabbit Corneas

At all times, the rabbits were housed and treated in accordance with the ARVO Statement for the Use of Animals in Ophthalmic and Vision Research. All experimental procedures were approved by the Committee for Animal Research of Kyoto Prefectural University of Medicine.

Using eight Japanese white rabbits weighing 2.4 to 2.8 kg (OBS, Kyoto, Japan), we performed superficial lamellar keratectomy to remove the entire corneal epithelium. To ensure complete removal of the limbal epithelium, we surgically excised the entire limbal epithelium and surrounding conjunctival tissue up to 2 mm from the limbus from one eye, down to the bare sclera. The cultured HCjE sheets were transplanted onto the denuded ocular surface to completely cover the resected area and were sutured in place with 10-0 nylon (8–12 sutures per sheet). The graft was then covered with a soft contact lens secured with four peripheral anchoring sutures. Finally, tarsorrhaphy was performed with 6-0 nylon sutures (Fig. 1B). After surgery, the rabbits were treated with topical antibiotics (0.3% ofloxacin ointment; Santen Pharmaceutical Co., Ltd, Osaka, Japan), triamcinolone acetonide (0.2 mL injected subconjunctivally; Bristol-Myers Squibb Co., Tokyo, Japan), and systemic antibiotics (10 mg gentamicin/rabbit, delivered intramuscularly [IM]; Nacalai Tesque Inc. Kyoto, Japan). They also received a daily IM injection of 0.2 mg/kg of the immunosuppressant agent FK506[23] (Astellas Co., Ltd., Tokyo, Japan) to inhibit a possible xenogeneic reaction or nonspecific inflammation.

Slit Lamp Examination

On the day of transplantation and on the 4th and 14th postoperative days, the ocular surface of the eight transplant recipients was examined and photographed with a slit lamp biomicroscope (SL-1600; Nidek Co., Ltd., Aithi, Japan).

Tissue Preparation

Engrafted tissues were removed from the eyes of eight rabbits killed 14 days after transplantation. In vivo conjunctival tissues, cultivated HCjE cells, and transplanted conjunctival tissues were divided into two portions, one of which was embedded in optimal cutting temperature compound (Tissue-Tek; Sakura Fine Technical Co., Ltd., Tokyo, Japan) and snap frozen with liquid nitrogen for immunostaining analysis. The other portion was processed for electron microscopy (EM).

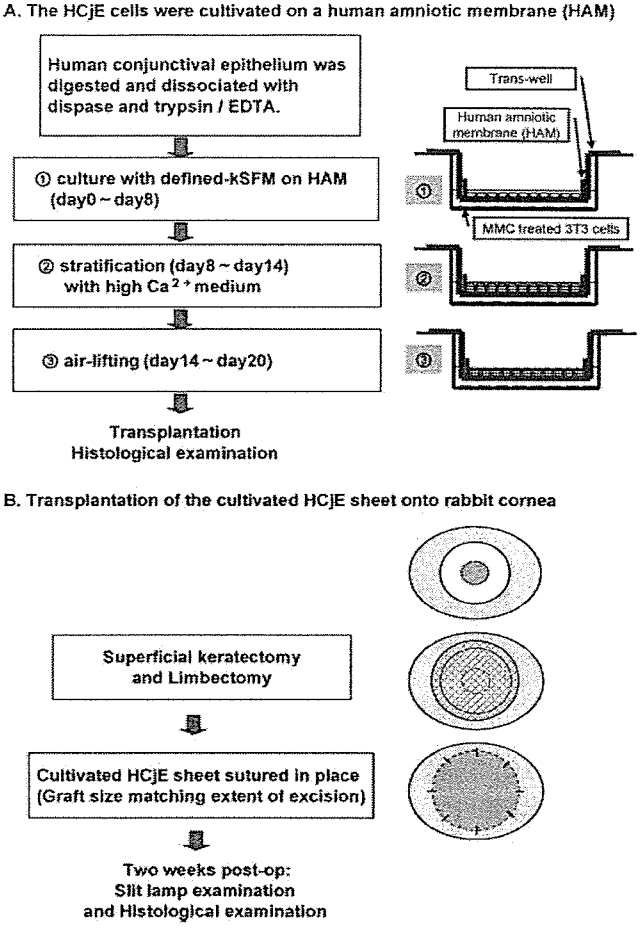

FIGURE 1. Cell culture of HCjE and transplantation into rabbit cornea.

Immunostaining and Light-Microscopic Analysis

Tissue sections (8 μm) were placed on glass slides and subjected to hematoxylin staining or indirect-immunostaining analysis. Briefly, the sections were fixed with Zamboni's fixative or acetone (4°C, 5 minutes), immersed for 1 hour in blocking solution (1% BSA in 0.01M PBS), and treated with primary antibody solutions (Table 1) and normal mouse IgG1, IgG2a, and IgG2b (Dako Cytomation Kyoto, Japan), and goat IgG (Santa Cruz Biotechnology Inc., Santa Cruz, CA) as the negative controls. After a 1-hour incubation, the sections were washed with 0.01 M PBS and then treated with fluorescent secondary antibody solutions (Alexa-488-labeled anti-mouse IgG or anti-rabbit IgG; Invitrogen, Carlsbad, CA). After 1-hour incubation, the sections were washed with 0.01 M PBS and mounted with medium containing an anti-photobleaching reagent (3% Dabco; Wako Pure Chemical Industries Ltd., Osaka, Japan). Fluorescent images of the sections were inspected and photographed with a confocal laser scanning microscope (TCS-SP2; Leica, Tokyo, Japan). Unless otherwise stated, all incubations were at room temperature.

Transmission Electron Microscopic Examination

Specimens were fixed in 2.5% glutaraldehyde in 0.1 M PB, washed 3 times in PB, and postfixed for 1 hour in 2% aqueous osmium tetroxide. They were then passed through a graded ethanol series, transferred to propylene oxide, and embedded in Epon-812 (TAAB, Berkshire, England). Ultrathin sections were cut and stained with uranyl acetate and lead citrate before examination under a TEM (H-7000; Hitachi, Tokyo, Japan).

TABLE 1. Antibodies Used in the Study

Group	Antigen	Dilution	Type of Antibody	Immunized Animal	Company*	Annotation
Putative stem cell markers	ABCG2	×40	(Mo)	M	Kamiya	ATP-binding cassette transporter
	p63	×100	(Mo)	M	Santa Cruz	p53 homologous protein
Adhesion molecule	Laminin5	×100	(Mo)	M	Chemicon	Hemidesmosome component protein
	Integrin α6	×100	(Mo)	M	Cymbus	Hemidesmosome component protein
	Integrin β4	×100	(Mo)	M	Chemicon	Hemidesmosome component protein
	Desmoplakin	×1	(Mo)	M	Progen	Desmosome component protein
Nuclei	Human nuclei	×30	(Mo)	M	Chemicon	Possible to distinguish human cells from other animal cells
Cytokeratin	CK3	×50	(Mo)	M	Progen	Major cytokeratin in corneal epithelium
	CK4	×100	(Mo)	M	Novocastra	Major cytokeratin in nonkeratinizing mucosal epithelium
	CK12	×100	(Po)	G	Santa Cruz	Major cytokeratin in corneal epithelium
	CK13	×200	(Mo)	M	Novocastra	Major cytokeratin in nonkeratinizing mucosal epithelium
Mutin	MUC4	×50	(Mo)	M	Zymed	A membrane-bound mucin
	MUC5AC	×100	(Mo)	M	Novocastra	Secreted mucin/goblet cell mucin

Mo, monoclonal; Po, polyclonal; M, mouse; G, goat.

* Kamiya: Kamiya Biomedical Company, Seattle, WA; Santa Cruz: Santa Cruz Biotechnology Inc., Santa Cruz, CA; Chemicon: CHEMICON International Inc., Temecula, CA; Symbus: Symbus Biotechnology LTD, Hampshire, UK; Progen: PROGEN Biotechnik GmbH, Heidelberg, Germany; Novocastra: Novocastra Laboratories Ltd, Newcastle, UK; Zymed: ZYMED Laboratories Inc., South San Francisco, CA.

RESULTS

Analysis of HCjE Sheets

HCjE sheets, grown on AM for 3 weeks, manifested five to six layers of well-stratified epithelium (Fig. 2A, 2D) without goblet cells (Fig. 2C). Thus, they were similar to in vivo corneal epithelium (Fig. 2B). The TEM examination revealed many microvilli on the surface of the superficial cells (Fig. 2E), desmosomes at intercellular junctions (Fig. 2F), and hemidesmosomes on the basal side of the basal cells (Fig. 2G).

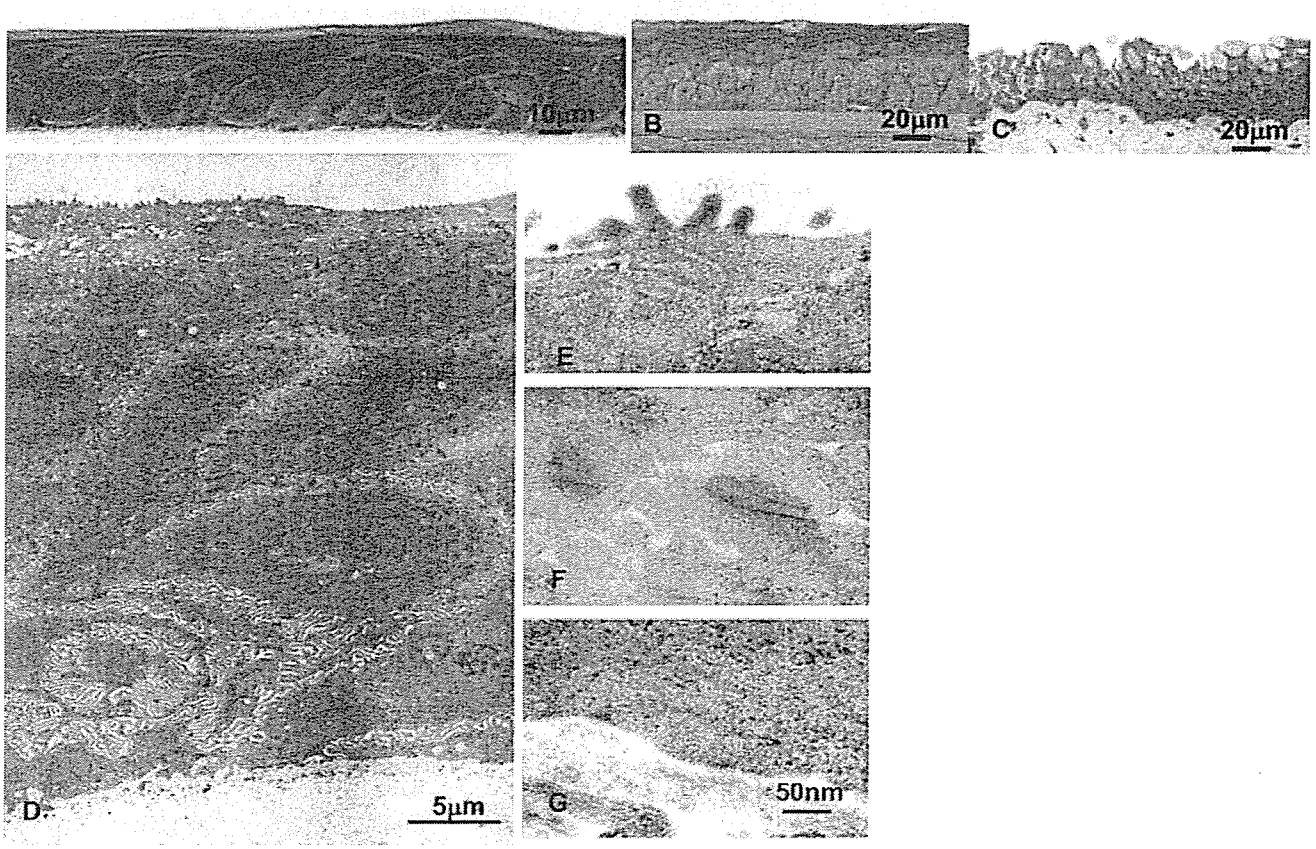

FIGURE 2. Histologic examination of HCjE cells grown on human amniotic membrane. Cultivated human conjunctival epithelium and in vivo corneal- and conjunctival epithelium were examined by light microscopy (A–C: semithin section stained with toluidine blue) or transmission electron microscopy (D–G). The cultivated epithelium was five to six layers thick (A, D) and exhibited typical microvilli (E), and desmosome- (F) and hemidesmosome (G) formation.

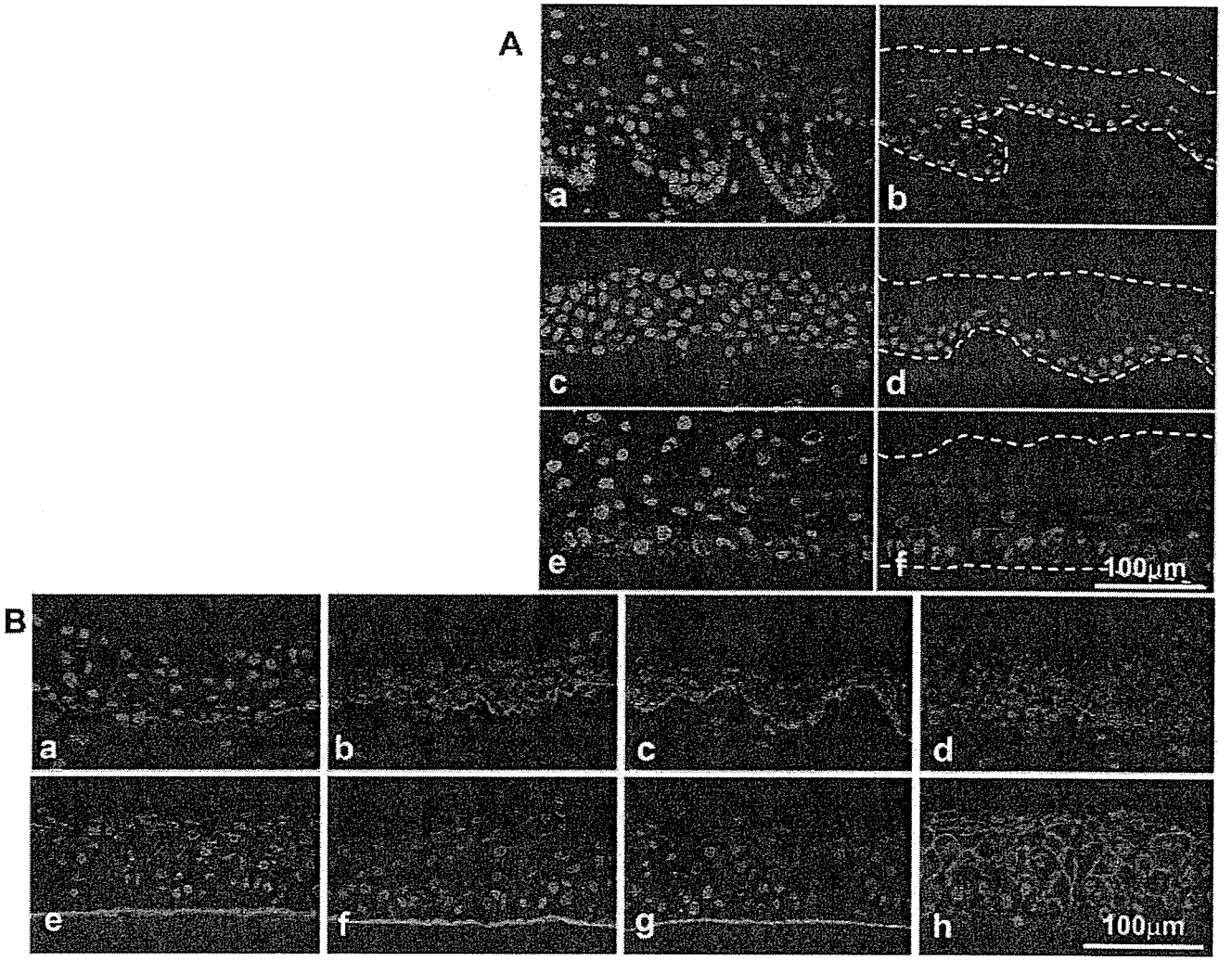

FIGURE 3. Expression of putative markers for stem/progenitor cells and epithelial adhesion molecules in the cultivated HCjE. (**A**) In vivo human limbal epithelium (**Aa**, **Ab**), in vivo HCjE (**Ac**, **Ad**), and cultivated HCjE (**Ae**, **Af**) were immunostained (*green*) with ABCG2 (**Aa**, **Ac**, **Ae**) or p63 (**Ab**, **Ad**, **Af**) and counterstained with propidium iodide (*red*). (**B**) In vivo HCjE (**Ba**, **Bb**, **Bc**, **Bd**) and cultivated HCjE (**Be**, **Bf**, **Bg**, **Bh**) were immunostained (*green*) with laminin5 (**Ba**, **Be**), integrin α6 (**Bb**, **Bf**), integrin β4 (**Bc**, **Bg**), or desmoplakin (**Bd**, **Bh**) and counterstained with propidium iodide (*red*).

Frozen sections of in vivo ocular tissues and cultivated HCjE were subjected to indirect immunostaining analysis. The basal cells of the cultivated HCjE sheets expressed the putative stem cell markers ABCG2 and p63 (Fig. 3Aa–Af); their expression patterns were almost identical with those of in vivo limbal epithelium. The hemidesmosome component proteins laminin 5 and integrin α6β4 were restricted to the interface between the basal cells and the AM. Desmoplakin, a desmosome-associated protein, was expressed at cell–cell borders. These expression patterns were almost identical with those of in vivo HCjE (Fig. 3Bg–Bn).

Transplantation of Cultivated HCjE Sheets

Cultivated HCjE sheets were successfully transplanted onto the cornea of all eight rabbits. The transplanted conjunctival epithelium completely covered all corneas and remained transparent, smooth, and devoid of epithelial defects during the 2-week postoperative observation period (Fig. 4). The transplanted HCjE was well-maintained on the recipients' corneal surface; there were no instances of graft retraction or dislodgement. The engrafted epithelium manifested five to six layers of stratified squamous epithelium, rendering it morphologically similar to normal corneal epithelium (Figs. 5A–D). We observed no goblet cells in the engrafted epithelium. As the grafts stained positive for the anti-human nuclei antibody that specifically reacts with human tissue,[24,25] we were able to confirm that the epithelial cells on the rabbit corneas were of human origin (Fig. 5E).

Histologic and EM Appearance of the Engrafted Conjunctival Epithelium

The engrafted epithelium consisted of five to six well-stratified layers harboring cuboidal or columnar basal cells, winged suprabasal cells, and flattened squamous superficial cells (Fig. 6A). There were many microvilli on the surface of the superficial cells. Tight junction-like structures were present at the cell–cell border of the superficial cells (Fig. 6B), and desmosomes were at the intercellular regions of the epithelial cells (Fig. 6C). Hemidesmosomes were seen at the basal cell-AM substrate junction zone (Fig. 6D).

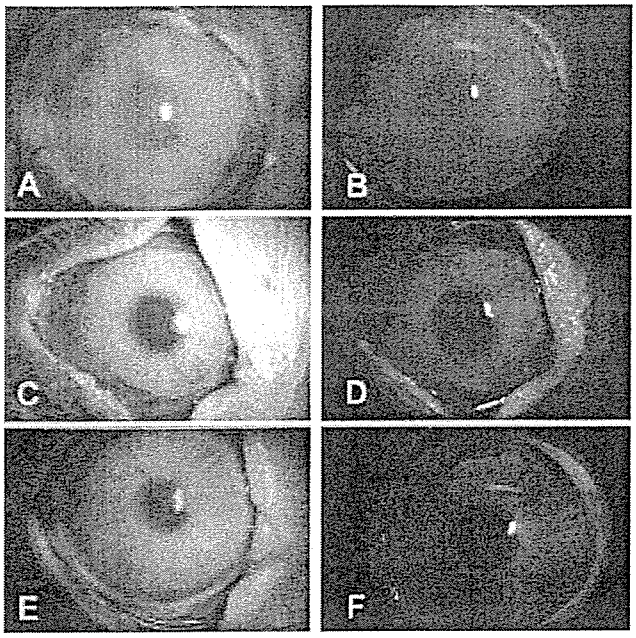

FIGURE 4. HCjE grafted onto the denuded rabbit cornea. The engrafted HCjE was inspected just after transplantation (A, B) and 4 (C, D) and 14 days (E, F) after transplantation. The engrafted HCjE was devoid of epithelial defects at all observation points.

Immunohistochemistry

Although MUC4 and MUC5AC were expressed by HCjE in vivo (Figs. 7A, 7D), neither cultivated nor engrafted HCjE cells stained positive for MUC5AC (Figs. 7E, 7F). In vitro cultivated HCjEs did not express MUC4, but engrafted HCjE was found to express MUC4 (Figs. 7B, 7C). CK4/13, normally expressed in conjunctival epithelium, was present in the cultivated HCjE sheets (Figs. 7G–L). In vivo conjunctival epithelium contained a few CK3/12-positive cells, as did cultivated and engrafted HCjE (Figs. 7M–R).

Discussion

We established a method for the culture of well-stratified conjunctival epithelium on human AM. The epithelial sheets we obtained exhibited high physical integrity, were well maintained after transplantation onto denuded rabbit corneas, and contributed to corneal transparency. Our results suggest that it may be possible to use these epithelial sheets for corneal epithelial replacement in patients with various ocular surface disorders.

It was initially intended in this study to culture rabbit conjunctival epithelial cells for transplantation onto rabbit corneas because this procedure is apparently free of undesirable xenogeneic rejection. However, the decision was made to transplant the cultivated HCjE sheets onto rabbit corneas for the following reasons. First, the optimal culture conditions for rabbit and human cells are reportedly different.[15,26,27] Consid-

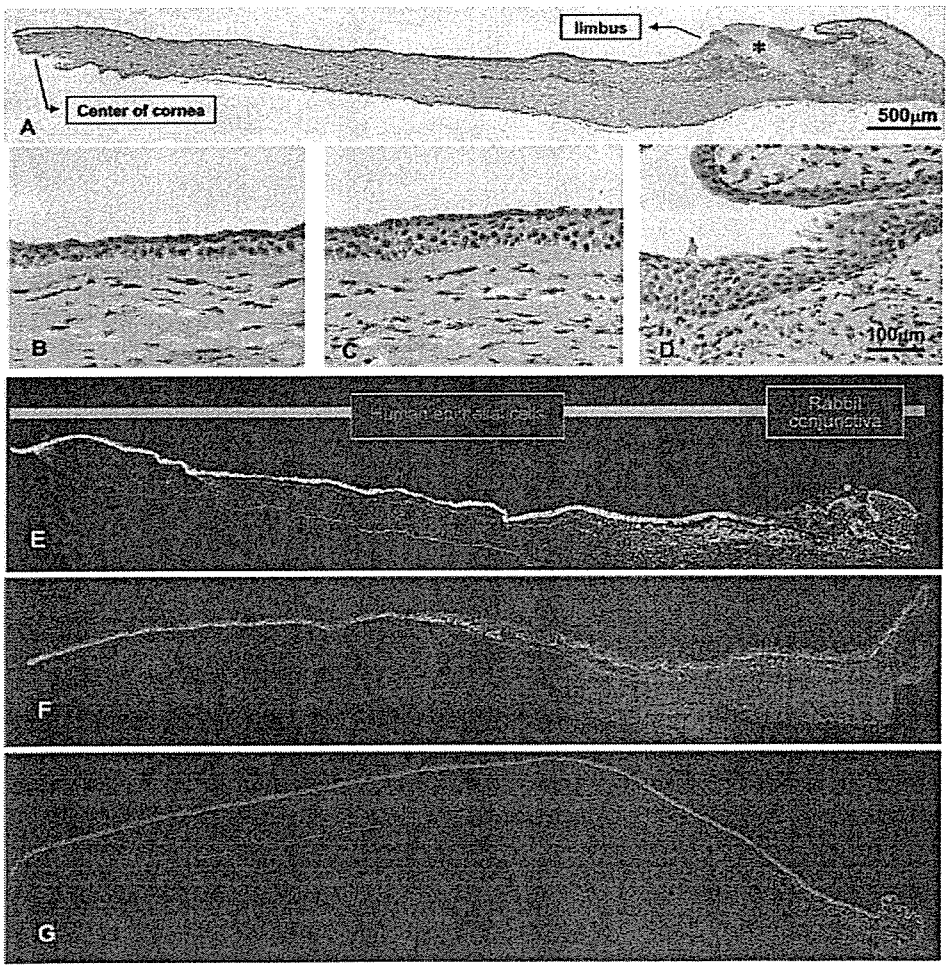

FIGURE 5. Light microscopy of the engrafted tissue and distribution of human epithelial cells on the graft. At 2 weeks, the engrafted epithelium demonstrated five to six layers of stratified squamous epithelium similar to normal corneal epithelium (A–C). (D) Conjunctiva of the recipient. No goblet cells were visible in the grafted epithelium (B, C). The engrafted cornea (E) stained positively with anti-human nuclei antibody (*green*). Normal human cornea (F) and rabbit cornea (G) served as positive and negative controls, respectively. The nuclei were counterstained with propidium iodide (*red*). (*) Suture track.

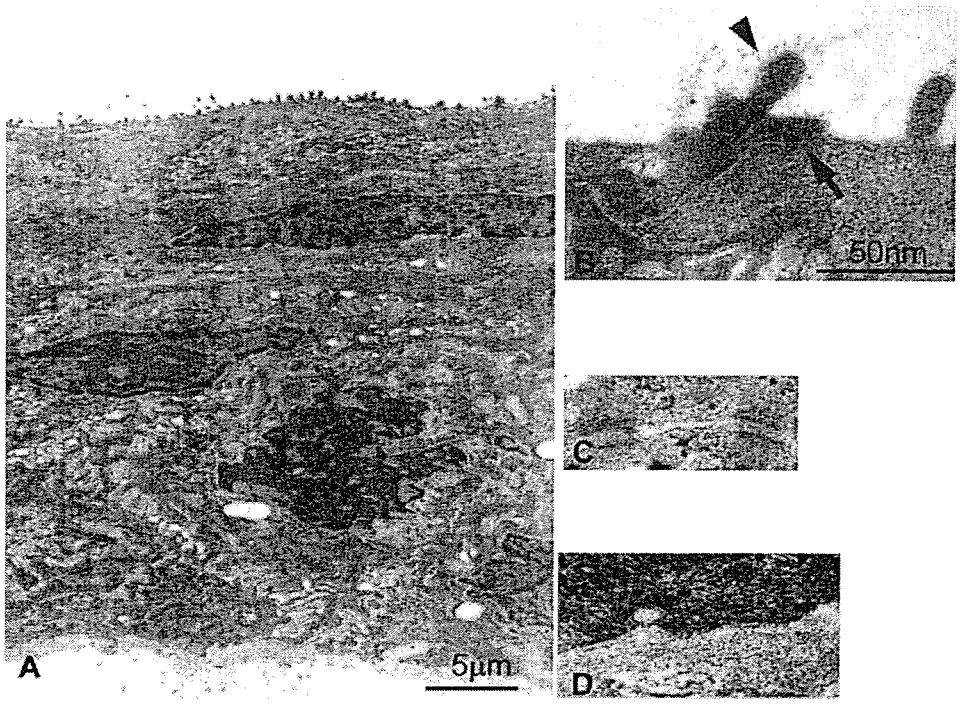

FIGURE 6. Transmission electron microscopy of the engrafted tissue. (A) Transmission electron microscopy at low magnification; (B) microvilli (*arrowhead*), tight junction (*arrow*); (C) desmosome (*arrow*); (D) hemidesmosome.

ering that our final goal is to translate our data to clinical treatment, it is crucial to determine the optimal culture condition for making well-stratified HCjE epithelial sheets which share sufficient physical integrity to tolerate intra- and postoperative surgical stress. Second, if cultivated rabbit conjunctival epithelium is transplanted onto rabbit corneas, it is difficult to discriminate between transplanted and migrated host-derived cells. In contrast, a great advantage of this experimental system was that the use of a specific antibody to human nuclei[24,25] made it possible to identify which cells were of human origin.

To ensure complete removal of the limbal and corneal epithelium, superficial lamellar keratectomy as well as complete limbectomy down to bare sclera was performed. Although we could not confirm that all the rabbit epithelial cells were removed, the expression of human-specific antibodies in the epithelial sheet helped to confirm that the epithelial covering was truly from the donor human tissue.

For the transplantation of HCjE to be successful, the cultivated sheet must possess structural integrity. The normal corneal epithelium features desmosomes at the cell- cell interface, and their presence contributes to its structural integrity. Hemidesmosomes at the basal cell surface serve to attach the basal cells to the underlying basement membrane. We demonstrated that desmosome-associated (desmoplakin),[28] hemidesmosome-associated (integrin $\alpha 6\beta 4$),[29] and basement membrane-associated (laminin 5)[30,31] proteins were present in the cultivated HCjE sheets. Furthermore, as in the corneal limbus, basal cells in the HCjE sheets expressed the putative stem cell markers ABCG2 and p63,[32,33] suggesting that they possess the structural and regenerative characteristics of corneal and limbal epithelium.[34]

MUC4, one of the mucin core proteins secreted from the surface of in vivo conjunctival epithelium,[6,35] was not expressed in the cultivated HCjE cells, although it was expressed in the engrafted HCjE. In rats fed a retinoic acid–depleted diet, the expression of mucin genes by the ocular surface epithelium was decreased.[36] Therefore, it is possible that the cultivated HCjE failed to express MUC4 because the culture medium lacked this solute factor. Alternatively, retinoic acid present in rabbit tears may have led to the recovery of MUC4 expression in the engrafted HCjE. MUC5AC was not found to be expressed in the goblet cells of conjunctival epithelium[37,38] in either cultivated- or engrafted HCjE, although a series of contiguous sections were inspected. Considering the previous report that approximately 500 goblet cells exist in a 1-mm^2 section of conjunctival epithelium,[39] 7500 goblet cells may exist in the initial period of cultivation. However, no goblet cells were identified, both in cultivated HCjE at the end stage of the culture and engrafted HCjE at 2 weeks after surgery. This suggests that our culture conditions did not support goblet cell differentiation in culture or after transplantation.

We recently reported that similar to corneal epithelial cells, as many as 1% of conjunctival epithelial cells are CK3/12 positive.[40] We postulate that the CK3/12-positive cells in the engrafted HCjE derived from the resected conjunctiva and were maintained in our culture system. We documented elsewhere[41] that the expression of thrombospondin-1, an inhibitor of vascularization, was much higher in corneal than conjunctival epithelium. As the expression level of this gene by CK3/12-positive cells in the engrafted HCjE was similar to the level seen in corneal epithelium, it may contribute to the inhibition of corneal neovascularization.

In patients with unilateral chemical or thermal injury, the conventional repair by limbal autografts from the contralateral eye requires 3 to 6 hours, and this may inflict iatrogenic limbal stem cell deficiency on the donor eye. The transplantation of autologous cultivated limbal stem cells has yielded promising results and requires the harvest of much less tissue, thereby reducing the risk of iatrogenic injury to the donor eye.[8,42,43] To treat bilateral ocular surface disorders such as SJS, our group has reported allogeneic transplantation[7] or more recently, autologous cultivated oral epithelial transplantation, as promising treatment options.[14,15] We now add cultivated autologous conjunctival epithelial transplantation for corneal epithelial replacement as a promising new modality to treat severe ocular surface disorders. It may be safer than the conventional methods currently used, and immunologically, it is superior to allogeneic transplantation. From a cytological point of view, autologous conjunctival epithelium represents a better alternative than oral mucosal epithelium for corneal epithelial replace-